DJO-1799

Design of a Ferry Kite Powered Water Pump

A Major Qualifying Project Report
Submitted to the Faculty of the
WORCESTER POLYTECHNIC INSTITUTE
in Partial Fulfillment of the Requirements for the
Degree of Bachelor of Science
in Mechanical Engineering

by

Megan Errichetti

Ronglin Na

Xiaozhu Liu

Zebulon Shippee

November 3, 2017

Approved by:

Professor David J. Olinger, Advisor
Mechanical Engineering Department, WPI

ABSTRACT

This project focuses on the continued design of the WPI Ferry Kite Powered Water Pump for use in developing regions with lack of clean water resources. A ferry kite is a fabric kite that moves up a second main kite line, beneath a larger delta kite. During a power phase, the rising ferry tensions a tether and transmits aerodynamic forces to a water pump mechanism on the ground. During a retraction phase, the aerodynamic forces are reduced, and the ferry falls down the main kite line in a controlled manner. A new ferry kite, with a stalling mechanism that can alter the ferry angle of attack between the power, retraction phases; was designed and fabricated. The water pump is placed on the ground to reduce the weight aloft and maximize wing loading. The ground system includes a rotary water pump, a bike wheel, a bike winch, priming system, and a retraction spring. Improvements of the system during this project include: design, fabrication and testing of two styles of ferry kites and multiple iterations of the ground system. Field testing was conducted on the new system, and basic operation of the ferry was confirmed. The new ground system was tested under laboratory conditions.

ACKNOWLEDGMENTS

This project would not have been possible without the guidance and expertise of several individuals. Professor David Olinger provided feedback on designs and assisted in our testing consistently throughout the project. We appreciate his dedication to renewable energies and value his knowledge in kite and wind power. Without him, this project would never have gotten off the ground. Furthermore, we would like to thank Don McCasland from the Blue Hill Observatory and Science Center in Milton, MA for allowing us to test at Blue Hills, for sharing his kite expertise, and for critiquing our designs. Jon Van Blarcum is responsible for the original conception and design of this kite system. We are grateful for his original work and guidance at the beginning of the project. Finally, we would like to acknowledge Erica Stults, WPI Information Technology Application Scientist, for helping the team decide how to best print our numerous 3D-printed parts and for working quickly to help our project progress.

AUTHORSHIP

This project is split into two teams: the air team and the ground team. The air team is comprised of Megan Errichetti (ME) and Rose Na (RN). The ground team is comprised of Xiaozhu Liu (XL) and Zebulon Shippee (ZS). Each team was responsible for certain areas of the project and writing the sections corresponding to their work. The rest of the paper is evenly distributed over the entire project team.

Table of Authorship

Section	**Author**
ABSTRACT	RN
ACKNOWLEDGMENTS	ME
AUTHORSHIP	ME
INTRODUCTION	RN
1 BACKGROUND	
1.1 Water Demand in Developing Nations	ME
1.2 Wind in Developing Nations	ME
1.3 Sustainability Demand	ZS
1.4 Airborne Wind Energy	ZS

1.5 Past Projects at WPI	XL
1.6 Project Goals	XL
2 DESIGN & METHODOLOGY	
2.1 Preliminary Field Testing	ME, RN, ZS, XL
2.2 Overview of Final Design	ME, RN, ZS, XL
2.3 Aerodynamic Design	ME, RN
2.4 Ground Pump Design	ZS, XL
3 RESULTS	
3.1 Aerodynamic Team	ME, RN
3.2 Ground Pump Team	ZS, XL
4 RECOMMENDATIONS & CONCLUSIONS	ME, RN, ZS, XL
4.1 Aerodynamic Team	ME, RN
4.2 Ground Pump Team	ZS, XL

TABLE OF CONTENTS

INTRODUCTION

The continued population growth throughout the world demands even more natural and energy resources. As the effective and economic power generation solution for rural and remote locations remains a challenge, regions in developing nations are facing even more significant difficulties. Since diesel power is expensive and hard to access, renewable energy becomes a more viable source of energy production. Researches over the past couple years have dramatically improved the efficiency and affordability of hydro, wind and solar power. Airborne wind energy, which uses kites to extract energy from the wind, has merged as one possible technology for use in underdeveloped nations.

The WPI Kite Power Project was initiated to develop a low cost kite powered energy generation system for use in underdeveloped nations. Various designs have been studied by thirteen different project teams, contributing to components of the system. The Rocking Arm and Rotary Kite-powered Water Pump design have been improved in its performance, safety and efficiency throughout the years. The system uses a rotary power pump to convert the circular motion of the unraveling tether into linear motion of the piston pump. The design successfully operates the water pump and water flow rates were measured for the final design. A new concept of ferry kite design was first studied by Jon Van Blarcum (2017) at WPI. Therefore, our team is aiming to explore the various options of ferry kites, initiate designs and improvements on Jon’s Collapsible Kite Powered Water Pump system. Since low altitude wind is often unstable, a two kite system was designed to use one of the kites to maintain altitude when the other one goes through power and retraction phases to generate usable energy. By translating wind energy directly into usable kinetic energy, in this case to power a water pump, the energy loss during kinetic energy and electricity conversion is eliminated. The power generation system could also be easily modified to operate any other mechanical device that requires basic kinetic energy to free manpower into something more efficient.

The goals of our project were to initiate design changes and iterations to the system that improve performance and reliability. The commercial popper kite provided unreliable lift and power phases. It was in need to be improved or replaced. A smoother resetting process to set the popper/ferry kite from retraction phase to power phase was necessary to be established. The oil pump in the Collapsible Kite Powered Water Pump system was replaced by a water pump that the frame of the ground system needed to be refitted, adding parts to avoid tether string slipping. A bike winch was added to reduce the retraction force and improve the power transmission in the lift phase. The initial bike crank was in need to be replaced to match the bike chain and pump-gear interface was crucial to complete the power transmission system. A priming system was also essential for the pump to function.

The team accomplished these set goals by extensive field testing and altering variations of designs. Final designs for each goal were reached through multiple iterations of design edits and cooperation with all team members. Designs were initiated by each member to optimize the older system. Each part was fabricated then tested in the lab to ensure operation. Final field testing was conducted to confirm functionality.

1 BACKGROUND

1.1 Water Demand in Developing Nations

Water scarcity in developing nations is often a concern. It currently affects more than 40 per cent of the global population, and it is still rising (United Nations, 2017). Some nations face physical water scarcity, due to limited physical access to water. Many developing nations face water scarcity due to economics. Economic water scarcity occurs in areas that cannot afford to retrieve water that is available, often due to expensive infrastructure. Areas that suffer from this form of water scarcity the most are portions of Central and South America, Central Africa, India, and Southeast Asia. (The Water Project, 2017)

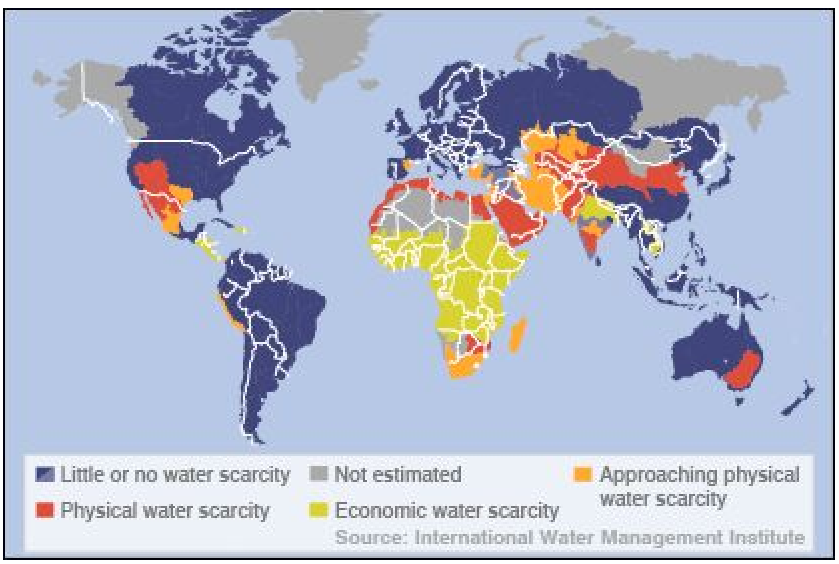

Figure 1: Water Scarcity Locations Around the World (The Water Project, 2017)

According to the Health and Medicine Division of the National Academies of Science, Engineering, and Medicine, an adequate amount of water intake is 3 liters per day for males and 2.2 liters per day for females. Assuming each member of a 100 person community needs 3 liters of drinking water per day, this community will need 300 liters per day. According to the World

Health Organization, 20 liters of water per person a day should be available to ensure that basic hygiene and food hygiene can be taken care of. A 100 person community will require an additional 2000 liters of water a day. In total, this 100 person community needs 2300 liters of water per day for drinking, cooking, and hygiene. Water scarcity is depriving communities not only of drinking water, but the water they need to keep themselves clean and grow food.

1.2 Wind in Developing Nations

Wind energy is very attractive economically and it is a proven technology. Many developing nations have not yet utilized their wind resources due to a lack of expertise within the nation and a lack of finances. Other countries have taken the initiative to help develop wind energy technology in developing nations. Back in 2000, the German Government funded a wind-energy program called TERNA (Technical Expertise for ReNewable Energy Application). TERNA is an overseas aid program that supports grid connected wind park projects in Africa, Latin America, and Asia. (Abramowski & Posorski, 2000). More recently, in 2016, it was reported that the world's poorest countries had invested more money in renewable energy in 2015 than the richest countries. The majority of the investments can from China, India, and Brazil. (Johnston, 2016).

According to the American Kitefliers Association, most kites fly best when there are wind speeds are 5-25 mph. Certain kites, such as Deltas, Diamonds and Dragon kites, will fly well is winds approximately 6-15 mph, while other kites, such as Box Kites and stickless Parafoil kites, will fly better when the winds get a little stronger, to approximately 8-25 mph. The final system developed in this project uses a delta and diamond kites. The wind speeds desired must be approximately 6-15 mph, which translates to 2.7-6.7 m/s. In the figures below, there are two maps: the average wind speeds in Africa and India.

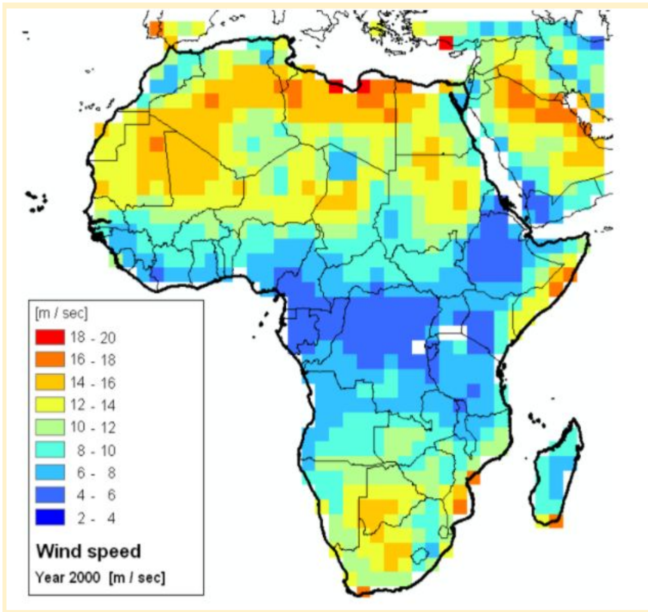

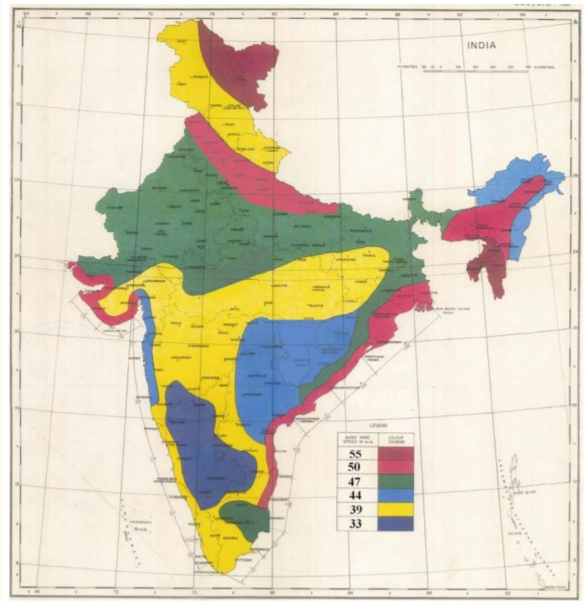

Figure 2.a:
Average Wind Speeds in Africa in m/s
(Bartholomė & Belward, 2013)

Figure 2.b:
Average Wind Speeds in India in m/s
(N. Lakshmanan, S. Gomathinayagam)

Africa displays average wind speeds most commonly between 2 and 10 m/s which would be ideal for a kite system. India displays larger wind speeds, with most being between 39 and 47 m/s. These wind speeds are high enough to power our kite system as well as larger kites. There is ample wind to power energy systems in these developing nations.

1.3 Sustainability Demand

The primary reason for developing a solution based on renewable energy is to combat climate change. The result of excessive amounts of greenhouse gas emissions trapping greater amounts of solar radiation, one serious threat of climate change is drought. As global temperatures rise periods of water shortage worldwide are becoming longer, more common and/or more substantial. Another, more obvious threat of climate change is hotter weather (Allen et al., 2010, Abstract section). According to the Occupational Safety and Health Administration

(OSHA) workers under dangerously hot and humid conditions may require as much as 4 cups of drinking water per hour to prevent ailments due to overheating and dehydration (Occupational Safety and Health Administration, n.d.), thus increasing local water demand. With these threats in mind, the ideal solution to lack of access to clean water will not increase greenhouse gas emissions as increased global climate change will create conditions where water is both less accessible and needed in higher amounts - exacerbating the very problem meant to be solved.

Another factor to consider is the high demand for renewable energy in third-world countries. According to Cassie Werber of Quartz Media LLC, “Developing nations invested $156 billion in renewables in 2015—a 19% increase on the year before, and more than all richer nations combined” (Werber, 2016). The main reason for this is that third-world nations have “a greater need for new energy capacity, and more flexibility in how to obtain it, because the lack of existing infrastructure can allow new systems to develop” (Werber, 2016). Therefore, developing countries are an ideal place to install renewable systems. Not only will it be an easier path to start toward reducing greenhouse gas emissions, but proving these technologies in low-tech environments with minimal resources could help further convince more wealthy and advanced nations of their potential viability.

1.4 Airborne Wind Energy

According to Moritz Diehl, “wind power is one of the few renewable energy resources that is in principle large enough to satisfy all of humanity’s energy needs” (Diehl, 2013). One promising version of this renewable energy source is known as Airborne Wind Energy (AWE). AWE refers to a method of harnessing wind energy via an airborne capture device rather than a ground-based static one as with conventional wind power. As such, AWE can access winds at much higher altitudes that generally blow more constantly and forcefully. Another important advantage to consider is that airborne wind energy systems can require fewer materials to construct relative to their power output than others systems. While conventional wind turbines require a tall rigid structure to access wind resources, AWE systems need only a collection device that can remain aloft, a base and a cable and/or tether connecting the two (Diehl, 2013). Depending upon the location within the system of the generator (or pump in our project's case) Diehl groups energy-producing AWE systems into two categories: “on-board generation” and “ground-based generation” (Diehl, 2013).

On-Board Generation

On-board generation AWE systems incorporate the generator within the airborne part of the unit. The simplest examples of this concept use a balloon's buoyancy to keep the turbine aloft. Altaeros Energies, for instance, designed a balloon that houses a turbine in its center and has a shape that provides some supplementary aerodynamic lift (see figure 3).

Figure 3: Altaeros Energies Buoyant Airborne Turbine or “BAT” © (Altaeros Energies, 2014).

Other designs, like those under exploration by Sky WindPower, equip the airborne part with a series of turbines that consume a portion of the energy that they harness to keep the apparatus in the air (see figure 4).

Figure 4: Sky WindPower Flying Electric Generator © (Sky WindPower, n.d.).

Alternatively, turbines may simply be attached to a kite that is held in the air by the same wind that it harnesses. If these do have powered moving parts, they are primarily for steering and/or takeoff (Diehl, 2013).

One technique for enhancing the potential of on-board generation AWE systems is what Loyd referred to as “crosswind kite power” (Diehl, 2013). By this technique, the airborne apparatus of an AWE system continually moves in a direction perpendicular to the wind from which it draws power. This additional vector increases the speed of the air relative to the apparatus, thus increasing the power it can draw with its turbines. With these higher wind speeds, the turbines also don’t need to rely on a bulky gearbox in order to attain the rotation speeds necessary for cost-effective power generation (Diehl, 2013).

Ground-Based Generation

Ground-based generation or Ground Gen AWE systems incorporate the generator at the base (Diehl, 2013). One type, called a “pumping mill” (Lansdorp & Ockels, 2005), operates using one or more kites attached to a tether which is wrapped around a drum at the base (Lansdorp & Ockels, 2005; Diehl, 2013).

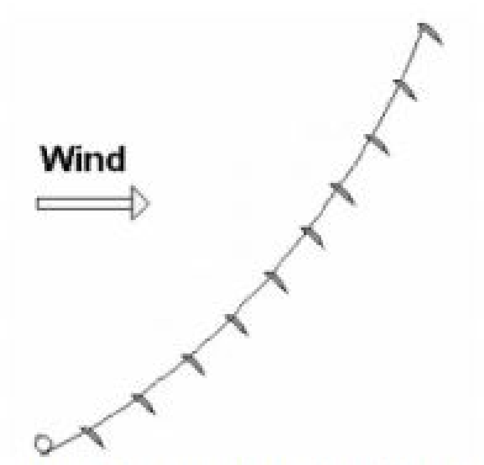

Figure 5: Generic diagram of a pumping mill (Lansdorp & Ockels, 2005).

As the kite flies out, it applies tension to the tether which unravels from the drum, resulting in useful rotation. After the kite flies out a certain distance, it is retracted back to its starting position to repeat the process. In order to yield a net gain in energy, the kite must reduce its drag and/or lifting force during retraction (Diehl, 2013). This is usually accomplished by changing its aerodynamics or by reducing its crosswind motion remotely - like with on-board generation, crosswind flight can improve power output for ground-based generation by increasing the air speed relative to the kite and by extension the tension in the tether (Cherubini et al., 2015).

One major advantage that ground-based generation systems have over on-board generation ones is that the tether does not need to transmit power down to the base (Diehl, 2013). This reduces power loss due to electrical resistance and the need for wider tethers that have lower electrical resistance and higher mechanical resistance. Furthermore, this configuration eliminates the need for power converters built into the kite which would make it heavier (Diehl, 2013).

Our design

Ultimately, the decision was made to use a Ground Gen system for the design. The ground-based generation system allowed for the captured energy to be transferred directly to the pump for maximum efficiency. Had an on-board generation system been used, installing an electric turbine in the kite would have resulted in considerable power loss along the tether between the kite's generator and the pump on the ground and at the energy conversion stages from kinetic to electric and back to kinetic. Attaching the turbine directly to the pump with this setup would also have been impractical given the need for a kite that could support the weight of the turbine as well as the pump, its pipes and the water running through them.

1.5 Past Projects at WPI

The kite power project at WPI advised by Professor David Olinger started around 2007 and was initially designed to generate electricity for developing countries (Blouin et al., 2007). The original design drew inspiration from an oil pump jack and had a pivoting beam which was set on the top of an A frame. The kite was tied at one end of the beam so that when the kite was moving up, it would pull the arm up and drive the generator. Springs set at the bottom could help to retract the string and pull the beam back.

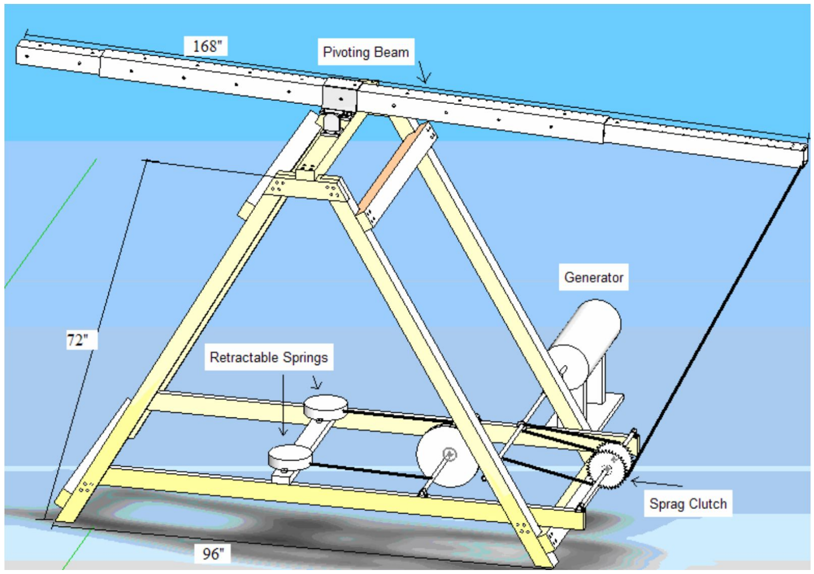

Figure 6. A Frame Kite Power System in 2007

Since the primary design was used, some improvements have been made to the prototype. A kite control system was built in 2008, which helped to keep the kite in the air for several minutes (Buckley et al., 2008). In 2009, A secondary power system was installed and improved the efficiency of the system (Alex et al., 2009). Meanwhile a newer oscillation controller was built to handle any the sudden force generated by the kite. In 2010, several modifications were made including adding a dynamometer, improving the gear shaft, replacing the old kite by a larger sled kite, redesigning the sliding mechanism, and redesigning the locking system (Toydemir, 2010; Cartier et al., 2010). Finally a remote control system was developed in 2011 which allowed the length of the tether to be controlled (Frewin et al., 2011). All the modifications mentioned above were based on the prototype created in 2007 instead of changing any major concepts.

In 2012, the focus of kite power projects shifted to pumping water instead of generating electricity. In the 2012 model, the generator was replaced by a piston pump and an extra turbine was attached on the tether near the kite (Bartosik et al., 2012).

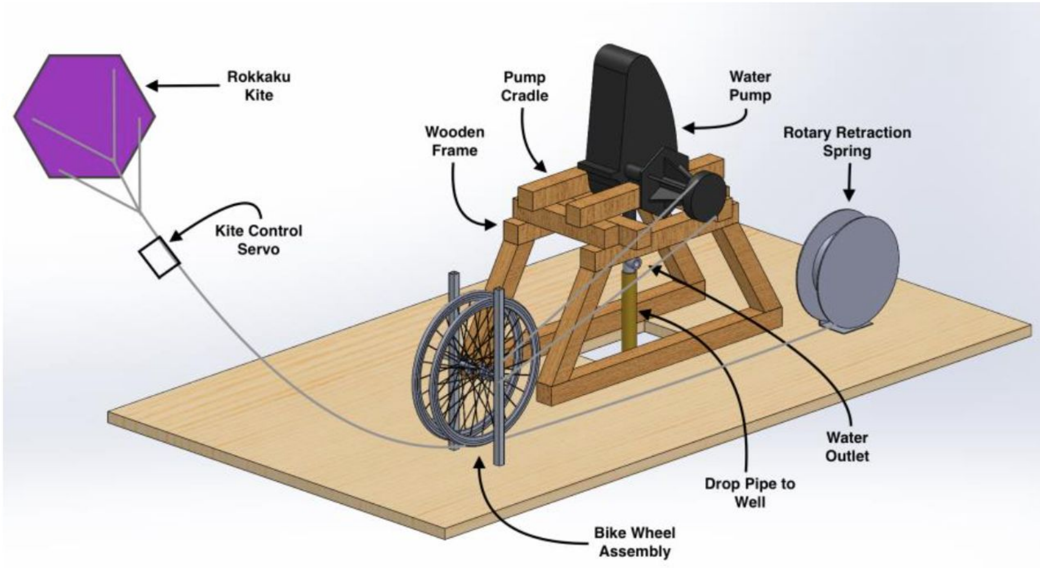

Figure 7. Rotary Kite Power System 2016 Summer

This rocking arm design remained until the kite spool idea came out in 2015. In the kite spool design, the linear motion which directly drove the piston pump was replaced by rotational motion (Chase et al., 2015). In 2016, the kite spool concept had been realized and improved by different teams. In the new design, the A frame was changed to a more stable structure with a lower center of gravity, two bike wheels were added, and a retraction spring was installed. The previously used piston pump was replaced with a rotary water pump, but it was still kept in the design as part of the priming system (Gagliano et al., 2016; Bauer et al., 2016).

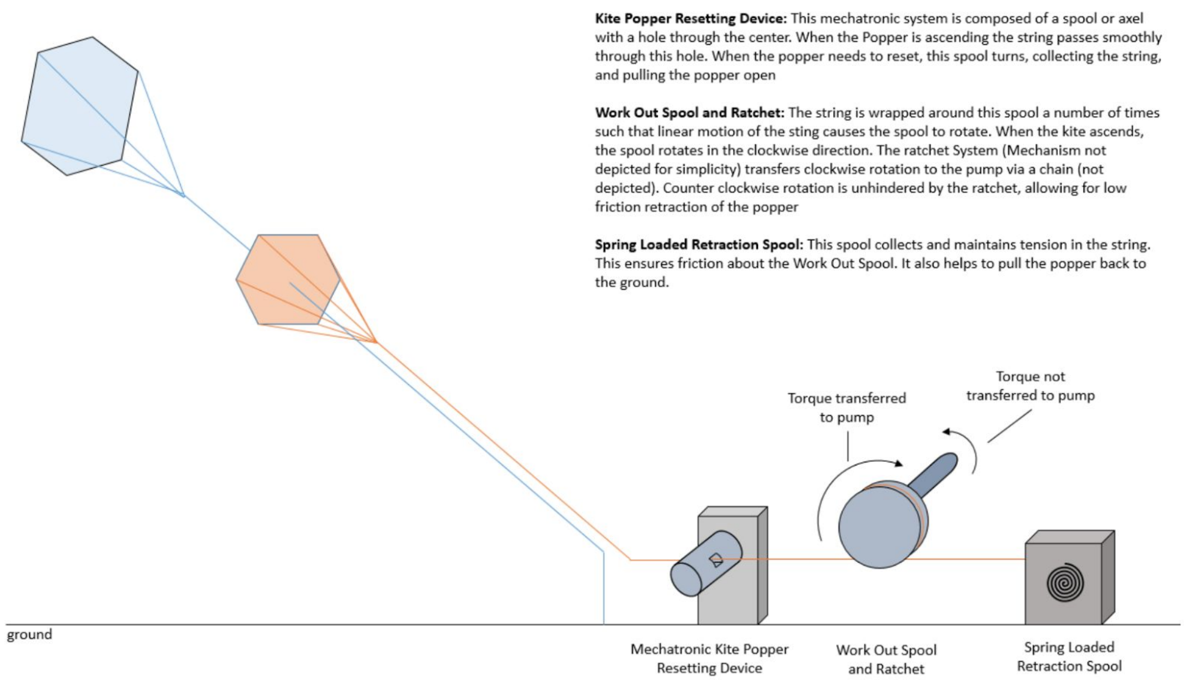

Figure 8. Kite power system from Jon Van Blarcum in 2017

Based on the 2016 MQP model, a more compact kite power system was created by Jon Van Blarcum (Figure 8). Compared to the early model in 2016, the design from Blarcum had a smaller rotary hand pump, only one bike wheel, and a retraction spring for the tether retraction (Blarcum, 2016). A more compact wooden frame was build due to the change in the size of each component. For the kite part, a Rokuku kite was used as the stationary kite and stayed in the air all the time while a collapsible kite popper would go up and down to pull the tether.

1.6 Project Goals

Project goals were developed and defined in the early stage and continuously updated to provide guidance in ensuring the proper focus and scope for this project. The team defined project goals as:

A. Develop a portable and sustainable Airborne Wind Energy Water Pump for use in developing nations

B. Continued development of the WPI Ferry Kite Powered Water Pump

Specific tasks were delegated to two teams, kite power team (air team) and ground team to better focus on separate issues and combine findings and designs for the final product.

The kite power team (air team) aims to improve the performance of the existing ferry kite power system by resolving the remaining problems and modifying the ferry. To be more specific, the project goals of the air team are to:

- Increase the surface area of the current popper design to maximize wind loading
- Design a more reliable Ferry Kite system to replace the kite popper and to include a stall mechanism to create effective kite power and retraction phases
- Conduct initial field tests for the new Ferry Kite to ensure functioning mechanism.

The ground team aims to improve the stability and efficiency of the existing power transmission system and to complete the piping system. To be more specific, the project goals of the ground team are to:

- Redesign the frame structure of the ground system to fit the reduction pulley and the relocated water pump.
- Find suitable bike crank for the chain and built the pump-gear interface.
- Design rollers to prevent the string from slipping off the bike wheel
- Design the bike winch to reduce the retraction force and prevent the tether from slipping on the bike wheel.
- Add a priming system for the water pump

2 DESIGN & METHODOLOGY

2.1 Preliminary Field Testing

When the initial prototype was first field tested at the Blue Hill Observatory and Science Center in Milton, MA on May 26 it was found that the bike wheel's design kept allowing the string to come off and tangle with the rest of the system. It happened so often that the string literally had to be retracted by hand to keep the system from jamming up. It was also found that the old metal pump had a tremendous amount of friction in it and its gear did not match with the chain in use. Additionally, the string wasn't actually attached to the bike wheel but merely wrapped around it. As such the transfer of motion from the string to the wheel - and by extension, from the kite to the gears and pump - was inconsistent as the string would slip somewhat along the edge of the wheel rather than maintaining traction.

The Kite Popper being used in the preliminary design of Jon Van Blarcum's Collapsable Kite Powered Water Pump project is a commercially designed and store bought kite designed by Peter Rondeau. In that system, the Kite Popper is designed to ride on the tether of the stationary kite and a knot on the tether line would hit the popper spur and stall the motion of the Kite Popper. The impact and the initial wind forces collapse the Kite Popper so that it falls back to its initial position as the retraction system picks up the loose Kite Popper tether line. As observed during the initial field testing, the Popper Kite only operates when it is directly facing the wind. It goes through a slow power and retraction phase. As it gets back to the initial position, the Kite Popper needs to be reset open to go back to power phase. In order to resolve the string tanglement with the knot and popper at the bottom of the stationary kite the following bead was designed to pass over the knot and tie to six expandable spurs. However, the whole popper was pulled towards one side due to the tether force direction, causing the system to fail.

2.2 Overview of Final Design

In this section, the basic operation of the WPI Ferry Ki8te Water Pump is discussed. Figure 9 shows the components of the new system designed in this project.

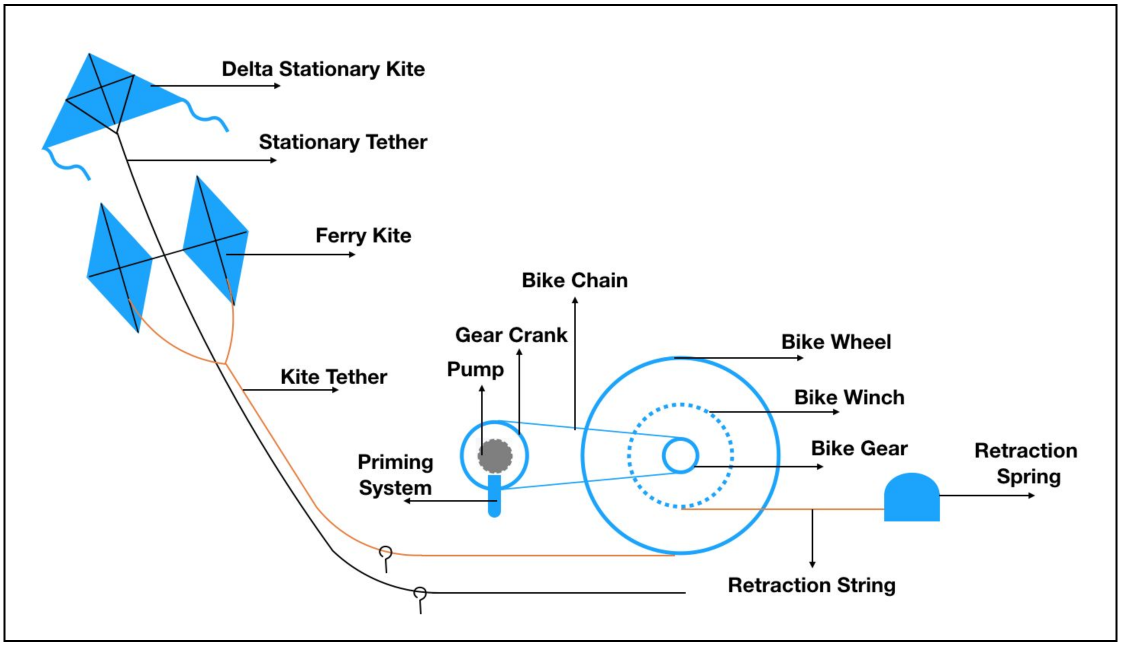

Figure 9: Final Design Overview

The heavier power generation mechanism and the water pump are designed to remain on the ground and separated from the kite system in the air. The kite system includes a 12-foot Delta kite and the improved Ferry Kite stall mechanism. The Delta Kite is a stationary kite that maintains altitude in the more stable wind and the Ferry Kite is designed to moves up and down the stationary tether, converting wind energy into kinetic energy. Water will fill in the hose by means of the priming system before the water pump starts operating. Wind pushes the ferry kite up the stationary tether as it pulls the kite tether that wraps around the bike wheel, which turns the gear crank that connects to the pump axle and pumps clean underground water. Then the Ferry Kite is designed to change its angle of attack, reducing the aerodynamic forces and falls down the main kite tether in a controlled manner. This controlled descent is an important new feature since lack of control of stalled kites during retraction phase was a serious problem with early designs. When the Ferry Kite comes down and is no longer able to drive the ground system, the retraction spring will turn the bike wheel and wrap the tether back on the wheel. Then the Ferry Kite will be reset and go through the same cycle.

2.3 Aerodynamic Design

In this section, the aerodynamic design is discussed in details. The theoretical analysis is firstly introduced to support the design decisions that are made during the process. The two different types of ferry kites and their design processes are presented as iterations of kites and their corresponding wind loadings.

2.3.1 Kite Aerodynamics

Stationary Kite

The forces that the stationary kite will be experiencing can be estimated by using a flat plate aerodynamic assumption. As seen in figure 1, the drag coefficients and lift coefficients are dependent on the angle of attack for a flat plate and can be estimated for the anticipated angle of attack.

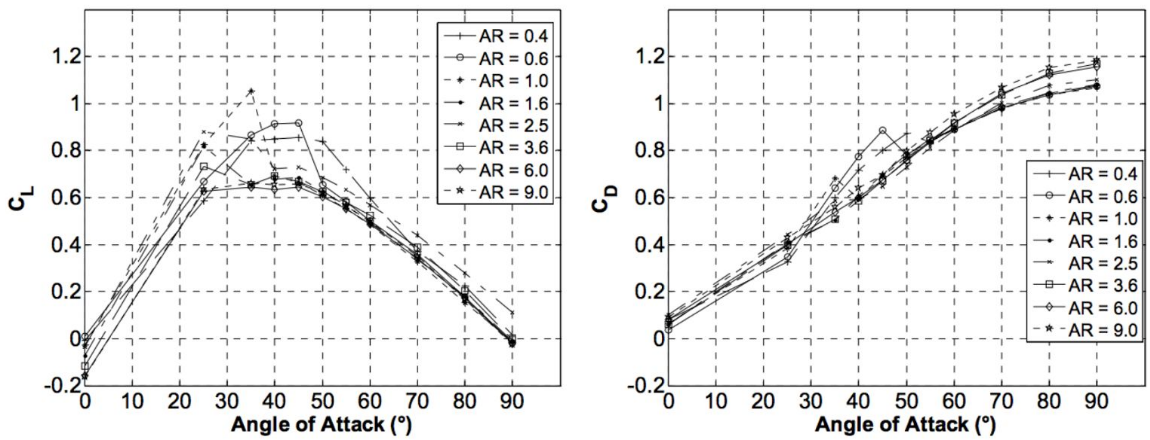

Figure 10: Lift and drag coefficients in relation to angle of attack in degrees.

For the stationary 12 foot Delta Kite, the anticipated angle of attack varies and the lift or drag force that acts on the kite depends on the angle of attack, as shown in Equation 1 and 2 below, where F_L and F_D are the lift and drag forces respectively. *A* is the projected kite area, ρ is air density, *v* is the free stream velocity, C_L is the lift coefficient, and C_D is the drag coefficient. However, the total force, shown in figure 2, is the total of the lift and drag forces, seen in Equation 3 below.

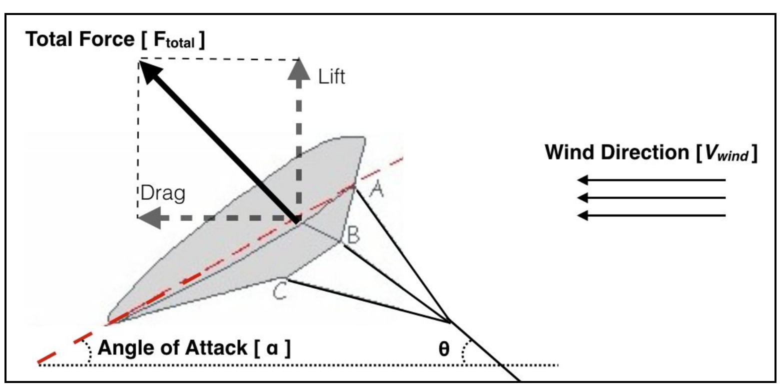

Figure 11: Force diagram on the stationary delta kite.

$$F_L = \tfrac{1}{2}\rho A v^2 C_L \qquad [1]$$

$$F_D = \tfrac{1}{2}\rho A v^2 C_D \quad [2]$$

$$F_{total} = \sqrt{F_L{}^2 + F_D{}^2} = \tfrac{1}{2}\rho A v^2 \sqrt{C_L{}^2 + C_D{}^2} \quad [3]$$

Due to constant air density at sea level, 1.225 kilograms per cubic meters, and constant kite area of the 12 foot Delta Kite, 8.28 squared meters, the total force on the stationary kite depends on the wind velocity and angle of attack.

The angle of attack is in relation to θ, the tether angle. Since the pump line will be parallel to the stationary tether, the tether angle will be the same for both the ferry kite that travels on the stationary tether and the stationary kite. The first order original angle of attack can be given as shown below in Equation 4.

$$\alpha_0 = 90 - \theta \quad [4]$$

Popper Or Ferry Kite Calculation

The popper is the kite that moves on the main stationary tether. It is directly attached to the ground system, going through a power phase and retraction phase to power the water pump. In order to maximize the force on the line during power phase, following analysis and calculation are performed.

The popper kite tether that is also attached to the pump is kept parallel to the stationary tether. The force diagram is shown in Figure 3 below.

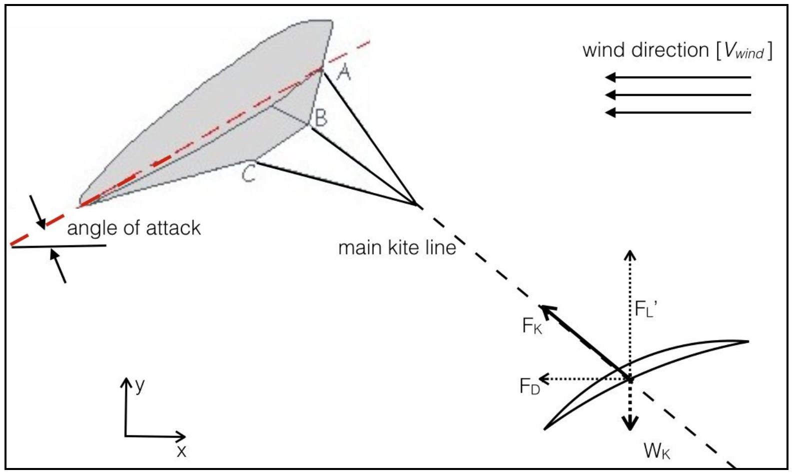

Figure 12: Popper force diagram in relation to stationary tether.

The popper experiences similar forces as the stationary kite from the wind. As the wind pushes the kite up during the power phase, the lift and drag on the popper follow the same equations as Equation 1, 2 and 3. The total force that acts on the popper is the sum of the lift, drag forces and the weight of the popper. With that being said, lift and drag depends on the angle between the kite surface and the wind as well as the lift and drag coefficients, which depend on the geometric property and the angle of attack. Due to the popper being a simple, thin, flat plate, the lift coefficient can be presented as shown below, where Cl_0 and C_{d0} are the first order ideas of the kite coefficients and α is the angle of attack.

$$Cl_0 = 2\pi * \alpha \quad [5]$$

$$Cd_0 = 1.28 * sin(\alpha) \quad [6]$$

However, as the popper moves up the stationary tether, the angle of attack also depends on the relative speed of the popper and the wind. The effective angle of attack gives more accurate lift and drag coefficients than the first order ideas.

The velocity vector diagram is shown below. As the wind speed is parallel to the ground and the kite speed is along the stationary tether, the angle between the kite velocity and the wind velocity is the same as the tether angle θ, shown in stationary kite calculation.

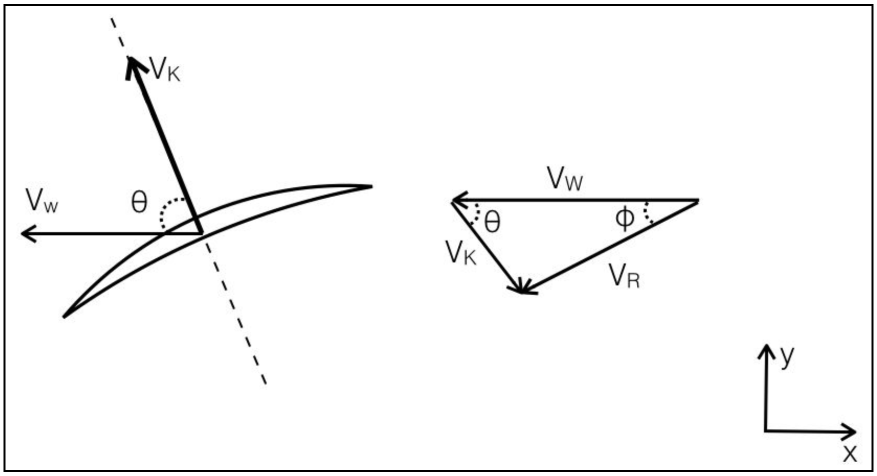

Figure 13: Velocity vector for popper

As shown in Figure 4, a moving kite experiences a relative velocity that could be represented by the velocity triangle, where V_w is the wind velocity, the V_k is the kite velocity and the V_R is the relative velocity.

$$V_R^2 = V_w^2 + V_K^2 - 2V_w \cdot V_K \cos\theta \quad [7]$$

$$\tan\varphi = \frac{V_K \sin\theta}{V_w - V_k \cos\theta} \quad [8]$$

Since the tether angle is known through field testing and experiments, the angle φ can be calculated. The effective angle of attack can be shown as below, where α_0 is the first order original angle of attack for the popper.

$$\alpha_{eff} = \alpha_0 - \varphi \quad [9]$$

Therefore, the more accurate lift and drag coefficients can be calculated to be input into Equation 1, 2, and 3 for the specific total force on the popper.

$$Cl = 2\pi * (\alpha_0 - \varphi) \quad [10]$$

$$Cd = 1.28 * sin(\alpha_0 - \varphi) \quad [11]$$

Furthermore, the total force on the popper depends on the original angle of attack in Equation 4. The following result is given by substituting Equation 10 and 11 into Equation 3.

$$F_{total} = \frac{1}{2}\rho A v^2 \sqrt{\left[2\pi * \left(90 - \theta - \frac{V_K sin\,\theta}{V_w - V_k\, cos\,\theta}\right)\right]^2 + \left[1.28 * sin\left(90 - \theta - \frac{V_K sin\,\theta}{V_w - V_k\, cos\,\theta}\right)\right]^2} \quad [12]$$

As shown above, the total force on the popper can be calculated as a function of air density (ρ), projected popper area (*A*), wind velocity (*v*), and tether angle (θ). Air density and wind velocity are largely depended on the experimental location and weather factors. Therefore, the variable that is concerned during the design process is the kite projected area. A table of the total force in relation to the projected area when the tether angle is 60 degrees is shown below.

Table 1: Varying Kite Area In Relationship With Force

C_L	C_D	V_w [m/s]	A_K [m²]	F_L [N]	F_D [N]	F_{tot} [N]
0.86	1.50	5.00	0.05	0.66	1.14	1.32
0.86	1.50	5.00	0.1	1.31	2.29	2.64
0.86	1.50	5.00	0.15	1.97	3.43	3.96
0.86	1.50	5.00	0.2	2.62	4.58	5.27
0.86	1.50	5.00	0.25	3.28	5.72	6.59
0.86	1.50	5.00	0.30	3.93	6.86	7.91
0.86	1.50	5.00	0.35	4.59	8.01	9.23
0.86	1.50	5.00	0.40	5.25	9.15	10.55
0.86	1.50	5.00	0.45	5.90	10.29	11.87
0.86	1.50	5.00	0.50	6.56	11.44	13.18
0.86	1.50	5.00	0.55	7.21	12.58	14.50
0.86	1.50	5.00	0.60	7.87	13.73	15.82
0.86	1.50	5.00	0.65	8.52	14.87	17.14
0.86	1.50	5.00	0.70	9.18	16.01	18.46
0.86	1.50	5.00	0.75	9.84	17.16	19.78
0.86	1.50	5.00	0.80	10.49	18.30	21.09
0.86	1.50	5.00	0.85	11.15	19.44	22.41
0.86	1.50	5.00	0.90	11.80	20.59	23.73
0.86	1.50	5.00	0.95	12.46	21.73	25.05
0.86	1.50	5.00	1.00	13.12	22.88	26.37

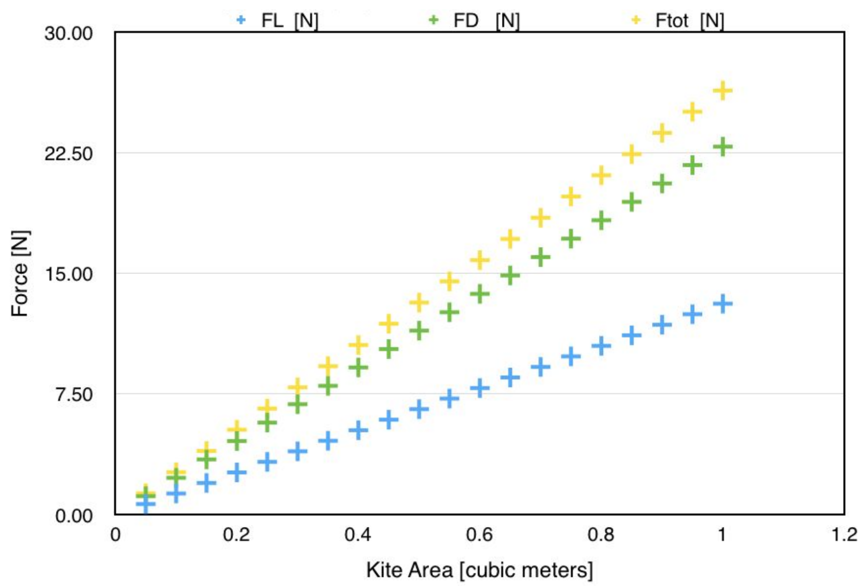

Figure 14: Total force on kite in relation to kite area

The linear relationship between the kite area and the total force acting on the kite is shown in the graph above. Therefore, once the ground team came up with a specific total load of ground system, the kite can be calculated to certain projected area to overcome the power generation load.

2.3.2 Popper

The first kite to be used for the kite powered water pump was a popper. A popper (figure 15) is a retractable kite. The popper rides up a stationary tether, which is the line attached to the delta kite. Near the end of the line, up by the delta kite, there is a nut tied on the line. When the popper reaches the nut, it is forced to a stop, and the wind forces the popper to close in on itself. Once the popper is closed, it falls down the stationary tether towards the ground where another nut tied on the stationary tether stops the popper. Another kite line, the popper kite tether, is attached to the 6 points of the popper using a 3D printed string organizer bead seen in figure 16.

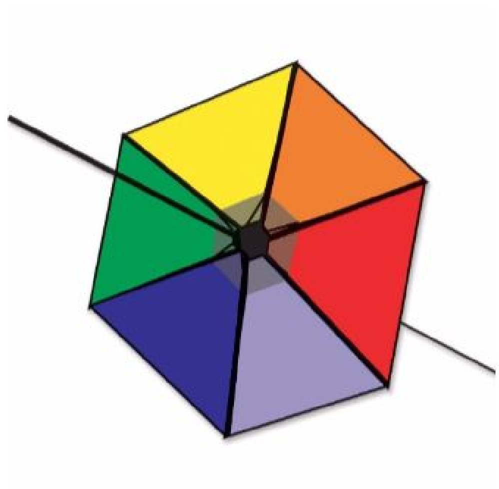

Figure 15: Premier Kites Popper Kite

The popper kite tether, which is attached to the string organizing bead at one point, can be pulled in order to reset the popper. Then the popper is free to go through this cycle again.

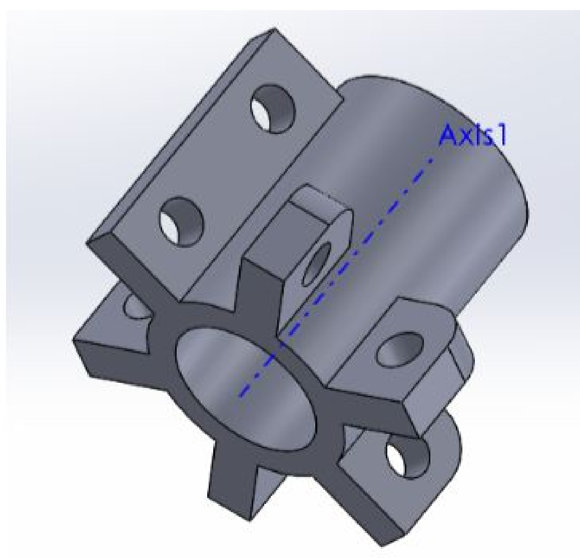

Figure 16: String Organizing Bead (Van Blarcum)

The popper kite tether is wound around a bicycle wheel that has a gear attached to its side. As the popper goes up the stationary tether, it turns the bicycle wheel, thereby converting its linear motion into angular motion. The gear attached to the bicycle wheel turns with the bicycle wheel and turns the pump.

Popper Wing Loading

Wing loading measures how much weight is supported by how large of an area. In the case of our kites, we want the wing loading to be a small number. We measured wing loading by dividing the total weight of the kite by its projected area.

$$Wing\ Loading = \frac{total\ weight}{projected\ area} \quad [13]$$

The projected area of the popper was measured by tracing the area of the open popper on the floor and measuring it there. The projected area has the geometry of figure 17 shown below. A scale was used to measure the mass of the popper -- the poles and fabric.

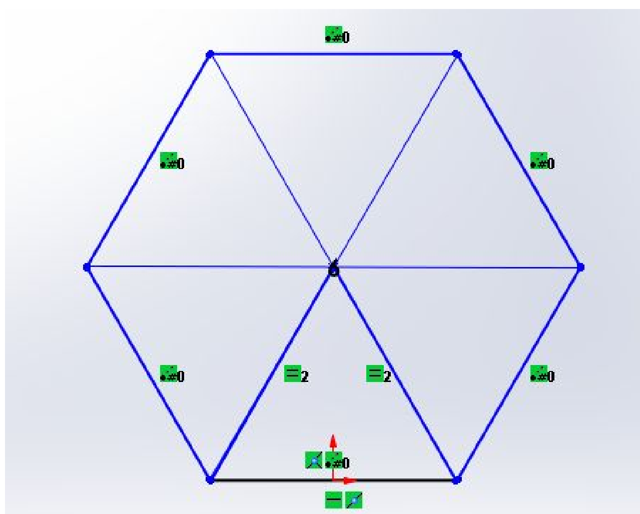

Figure 17. Geometry of Popper's Projected Area

The original popper that was used for testing in Van Blarcum's report is the largest commercial popper available. We traced the projected area of the popper onto the floor and measured one of the six triangular components. It's dimensions are shown below in figure 18.

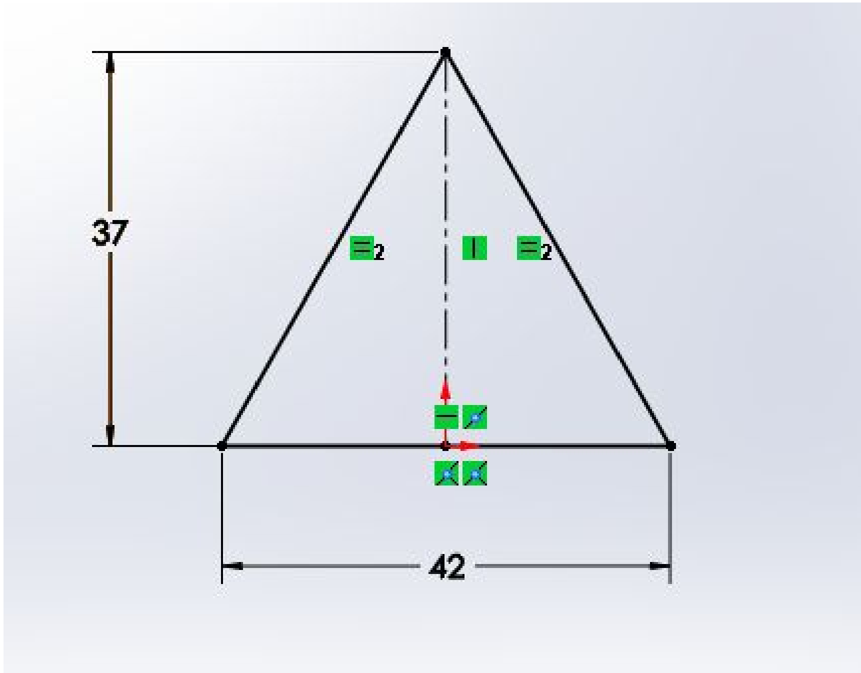

Figure 18. Triangular Section Measurements of Original Popper (measurement in cm)

The original popper's projected area is 0.0777 m^2. The mass of the original popper is 114.6 g. This converts to 0.1145 kg which can then be multiplied by 9.81 m/s^2 to give a weight of 1.124 N. The wing loading of the original popper is 14.47 N/m^2.

The first iteration of our expanded popper design used the original popper with 6 added poles branching off from the ends. The second iteration used the same pole set up, but used less fabric to create more tension at the ends of the poles. The second iteration popper's triangular dimensions are shown below in figure 19.

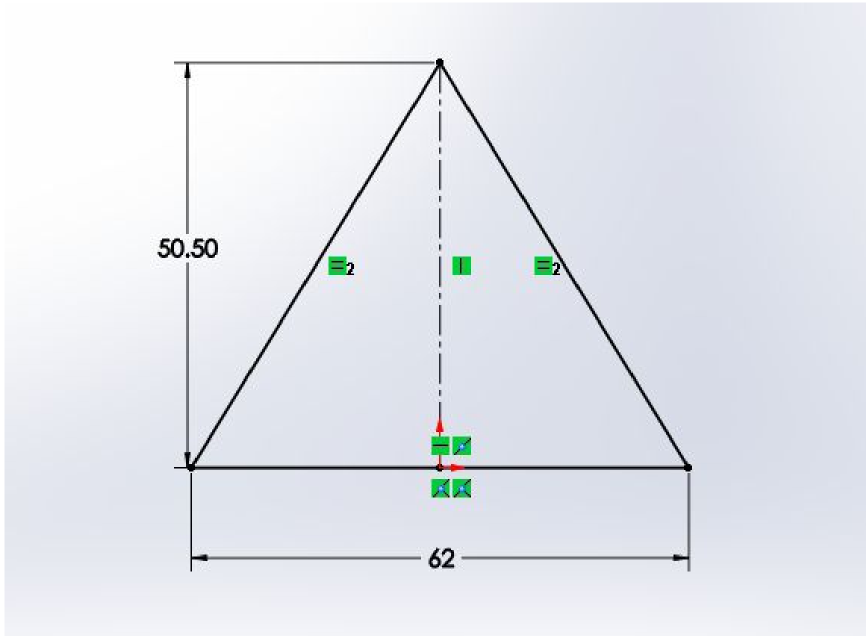

Figure 19. Triangular Section Measurements of Second Iteration Popper (measurement in cm)

The second iteration popper had a projected area of 0.9396 m^2. This popper had a mass of 306.2 g which comes out to a weight of 3.00 N. The wing loading of this popper is 3.20 N/m^2.

In the third iteration of the popper, we created a few insertions in the pole sleeves so that we could run a thinner, flexible pole along the whole length of the popper. The poles attached to the popping mechanism are still there, but we added new poles that run over the old poles all the way out to the ends. This reduced bowing in the popper, producing a larger projected area. The third iteration popper's triangular area is shown below in figure 20.

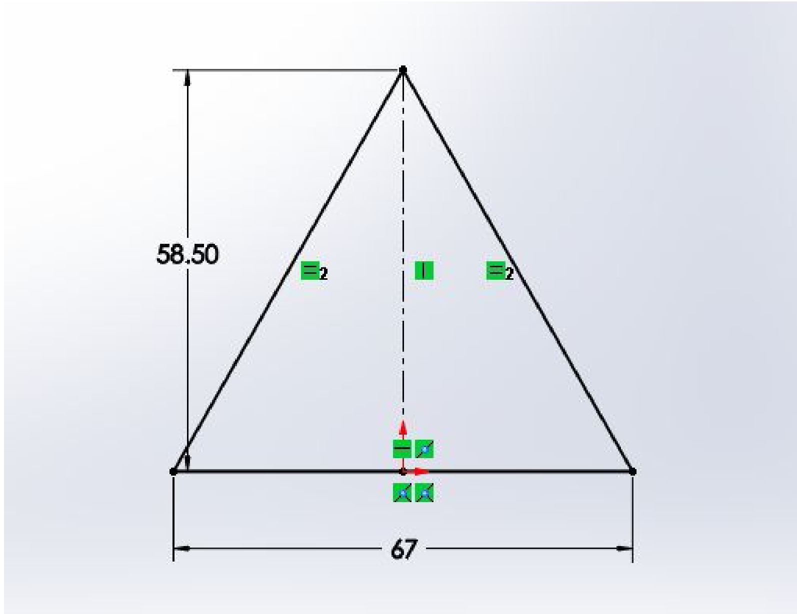

Figure 20. Triangular Section Measurements of Third Iteration Popper (measurement in cm)

The third popper iteration is the largest so far and has a projected area of 1.176 m^3. This popper had a mass of 270.1 g which comes out to a weight of 2.65 N. The wing loading of this popper is 2.25 N/m^2.

Each popper iteration had a lower, and thus better, wing loading. A summary of the wing loadings can be found below in Table 1.

Table 1. Wing Loading of Various Popper Iterations

	Wing Loading (N/m^2)
Original Popper	14.47
Iteration 2	3.20
Iteration 3	2.25

Popper Design Evolution

The original popper design is a commercially designed and store bought kite. This popper was used in Jon Van Blarcum's Collapsable Kite Powered Water Pump project.

In Van Blarum, 2017, it was recognized that there were issues with the current design recommendations were provided on how to proceed. The most immediate recommendation was to increase the kite surface area in order to increase the wind force being applied on the kite. So, in order to create the first iteration of the popper, the air team sewed on 6 new panels that extended off of the original popper. The popper with the 6 added panels is shown in the figure below.

Figure 21. First Iteration of the Popper (added panels)

The first iteration popper had such an increase in surface area that the projected area went from 0.0777 m^2 to 0.9396 m^2. 420 mm long poles were added to support and tension the new fabric. These poles were in separate sleeves than the poles of the original popper and were in no way attached to the original poles. The poles that were added were stiff, hollow poles with a diameter of 8 mm. The new fabric and poles were tensioned with arrow nocks that were attached to the ends of the poles and elastic cord that was sown onto the tips of the outer fabric.

Figure 22. Additional Support Poles to Support New Panels on First Iteration Popper

When we tested the first iteration of the popper, it did catch the wind effectively. The popper was barely able to move up the stationary tether. When the popper was in the popped position, the fabric was not tensioned enough. The team decided to try and tension the new fabric more. A picture of the first iteration popper field testing can be seen in the figure below.

Figure 23. First Iteration Popper Field Testing at Blue Hill Observatory

For the second iteration of the popper, the team created more tension for the outside fabric. We cut the outside fabric, overlaid it, and sewed it while the pieces were overlapping. The overlapping of the fabric can be seen in the figure below.

Figure 24. The Overlapping of Fabric for the Second Iteration Popper

This definitely created more tension within the popper. However, when the popper was in the pooped position, it now experience a significant amount of bowing. The popper in the popped position resembled an umbrella as can be seen in the following figure.

Figure 25. Second Iteration Popper in the Popped Position

When we tested this version of the popper, the wind had a hard time catching the popper in a uniform way. Instead of continuously going up the stationary tether, the popper would fall to one side and slide back down the stationary tether.

The team recognized that the second iteration had too much bowing. Additionally, we noticed that the thick poles that were added to the original popper were adding to the bowing effect since they were not connected to the original poles in any way. So, for the third iteration, we removed the thick poles from the first and second iterations, and replaced them with long, thin poles that were able to run the entire length of the popper, from the popping mechanism in the middle, to the elastic cord on the outside points of the popper. These poles were 710 mm long and had a diameter of 3 mm. By adding these thin, flexible poles, the popper was much flatter in the popped position. The figure below compares the new pole, bottom pole, to the pole used in the first and second iterations of the popper, top pole, when they are bent. The bottom pole is clearly significantly more flexible.

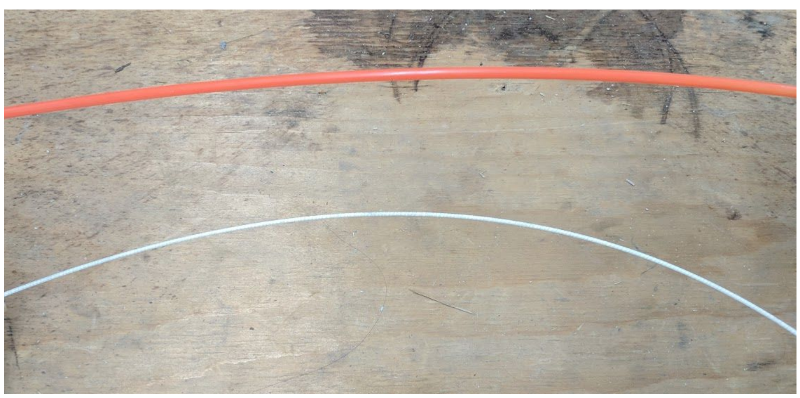

Figure 26. Comparison of Pole Deflection in Iteration 1 and 2 vs Iteration 3

We also removed the stitching that had overlapped the outside fabric in the second iteration of the popper and secured the fabric together normally. In order to give the added panels so more tension, we overlapped the very ends of the new panels a slight amount, but did not overlap the panels up by the original popper at all. This added the needed tension while also reducing the bowing from the previous iteration when the popper was in the popped position.

Figure 27. Third Iteration of the Popper in Popped Position

When the third iteration of the popper was field tested, it was able to move up the stationary tether better than the earlier iterations. However, it still experienced some issues with the wind pushing it to one side or the other instead of uniformly distributing. Unfortunately, one of the poles broke off from the popping mechanism in the middle of the kite at some point early on during that field testing day, so we were unable to fully test the third popper iteration.

Figure 28. Third Iteration Popper during Field Testing. The delta kite area is greater than the popper area.

Popper Resetting Process

As mentioned at the beginning of the popper section, the popper closes at the end of each power cycle. In order to be reset, the popper needs to be opened again. This is done with a motor set up between the kite and the bicycle wheel. The motor box has a spool with a small hole where the popper kite tether goes through. When the popper needs to be reset, the motor spins the spool which then pulls on the popper kite tether. The popper kite tether is attached to the popper with the string organizing bead. The organizing bead is tie to the six expandable spurs and to the stationary tether. There is another knot near ground on the stationary tether that would completely stop the popper. The organizing bead smoothly passes over the knot/stopper and lets the popper to come in contact with the stopper. By pulling the tether, the motor box pulls the popper against the stopper, re-opening the popper to initial state for the next power phase.

The motor and its circuitry are the same as what was used in the Redesign of the WPI Rotary Kite-Powered Water Pump MQP (Bauer, Beauchemin, Draper, Munene, Blarcum, Zhao, 2016). The circuit hooks up the motor to a remote controlled Arduino. The motor box and wireless capabilities allow us to pull on the popper to reset it while it is hundreds of feet in the air.

The problem with the resetting process is really just a problem with the string organizing bead. The string organizing bead connects all 6 pole points on the popper to the one popper kite tether. However, the popper kite tether is attached to the string organizing bead on one side. So, as the popper moves up and down the stationary tether, the popper kite tether is dragging the string organizing bead to one side along the stationary tether. This creates unwanted friction and slowly destroys the string organizing bead. The string organizing bead also needs to have a large enough hole in the middle so that the nut that is attached to the stationary tether can pass through it.

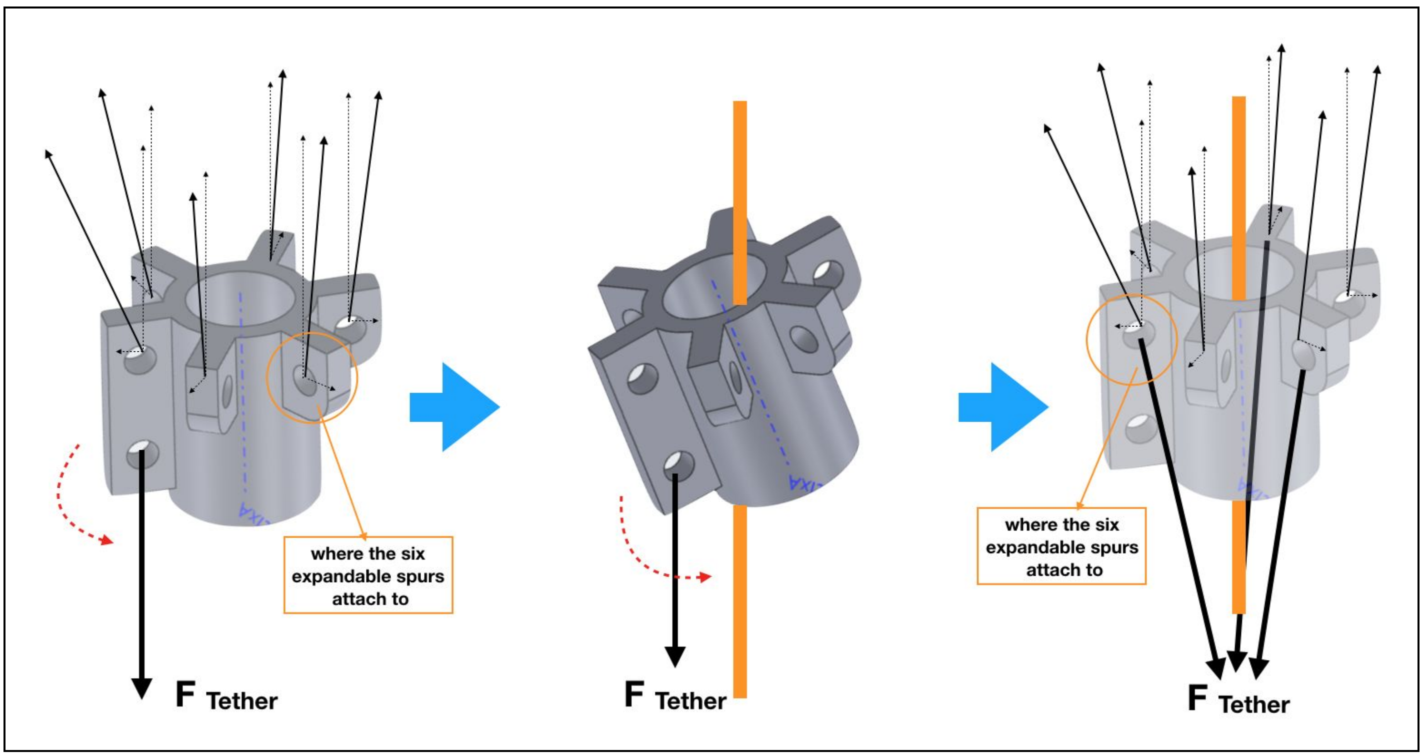

Figure 29: String Organizing Bead Force Diagrams

As seen in Figure 29, the original system on the left pulls the string organizing bead at one point. The single downward force cannot overcome all of the forces from the six expandable spurs and instead of pulling the whole string organizing bead downwards, the kite tether that is attached to the motor or the ground powering system introduces a force moment. Shown in the middle diagram where the orange line is the stationary tether that goes through the bead. The introduced moment tilts the bead that it rubs against the kite line and creates unnecessary friction. Each expandable spurs are tensioned the same on a popper, and the popper can only be pulled open if equal forces were applied. Since the six strings that are tied to the six expandable spurs are directly attached to the string organizing bead, circled in orange in the figure above, the tilted bead pulls one side of the popper more open than the other side. It caused difficulties and failures in the resetting process. As seen in the third diagram in Figure 9, the organizing bead could be balanced by introducing two more downward forces. When considering methods of introducing the forces, strings were eliminated to avoid string tangelments. 12 gauge copper wires were used to attach to the string organizing bead. The kite tether was directly tied to the three wires as shown in Figure 30 below.

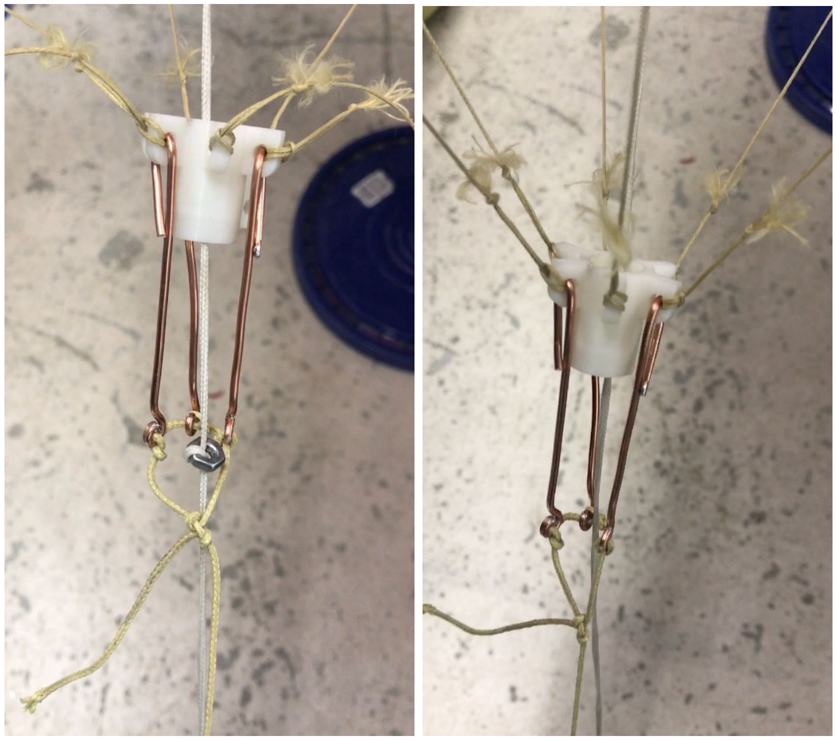

Figure 30: Final Design of the String Organizing Bead for Resetting Process

Attaching the three wires together, the kite tether forms a small loop that the stopper knot can pass through. By adjusting the position of each wire on the loop and tie it down, the wires are made sure to be pulling the organizing bead evenly. As seen in the picture on the right, the improvements effectively address the issue of tilting the organizing bead and causing the bead to come in contact of the stationary tether. The resetting process is in result more reliable. However, during the field testing for the process, the copper wires heated up quickly and became flexible that they were bent. For future usage, the wires could be replaced by more stable materials to guarantee performance.

2.3.3 New Ferry Design

Ferry Design Evolution

The Ferry Kite is designed to replace the popper kite with a more reliable mechanism that could easily support more kite surface area.

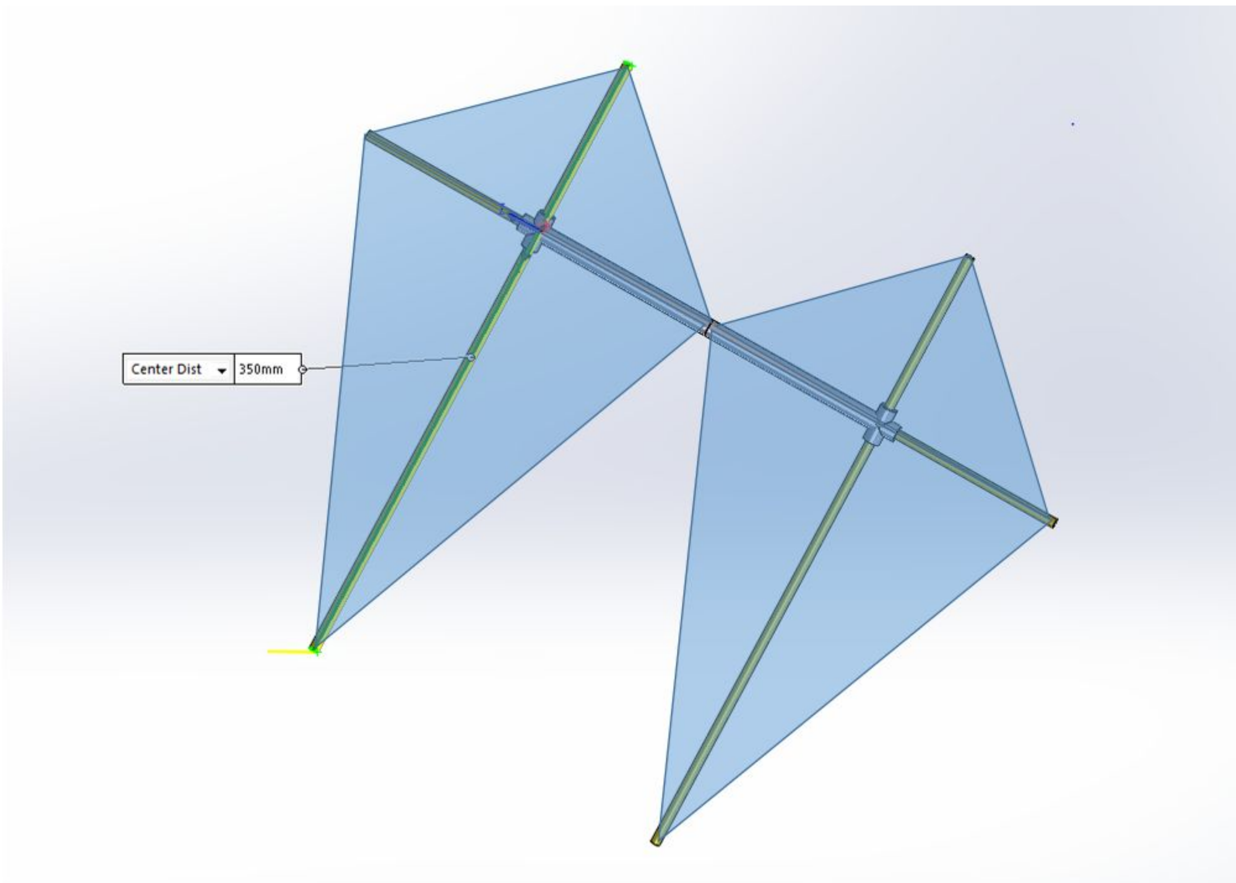

Figure 31: Ferry Concept

Similar to the Popper, the Ferry Kite will be sitting on the main stationary tether, pulling the power tether from the power generation system. The concept of the ferry is designed to be two diamond shapes that can be balanced on either side of the kite line. The kite fabric would be set to be perpendicular to the wind direction at initial state. It will be pushed along the stationary tether. A center mechanism is designed to change the angle of attack of the Ferry

Kite when the kite hits the stopper just below the main delta kite. The mechanism would turn the fabric of the kite to nearly parallel to wind direction in order to significantly reduce the wind force on the kite. The weight of the Ferry and the retraction system then assure Ferry Kite would fall back to the ground under the influence of gravity. The Ferry concept simplifies the resetting process since the ferry just needs to be pulled back to the initial starting angle of attack to transition into power phase.

For the first iteration, the Ferry Kite design included 7 orange stiff poles, 2 force-fit pole connectors, 2 one-inch-diameter gears, a corresponding rack, a quarter-inch dowel pin, two parts of center mechanism, rack support and main support parts. As shown in figure 32, the red highlight labels all the 3D printed parts.

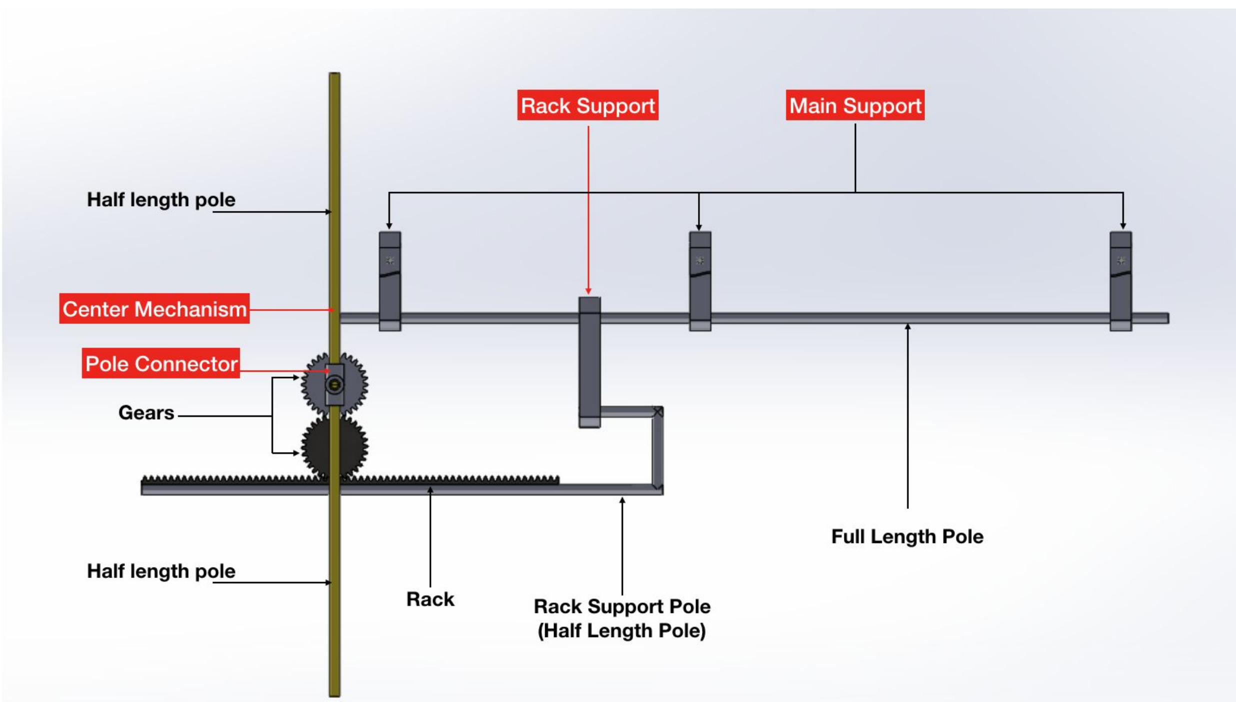

Figure 32: First Iteration Ferry Design Side View

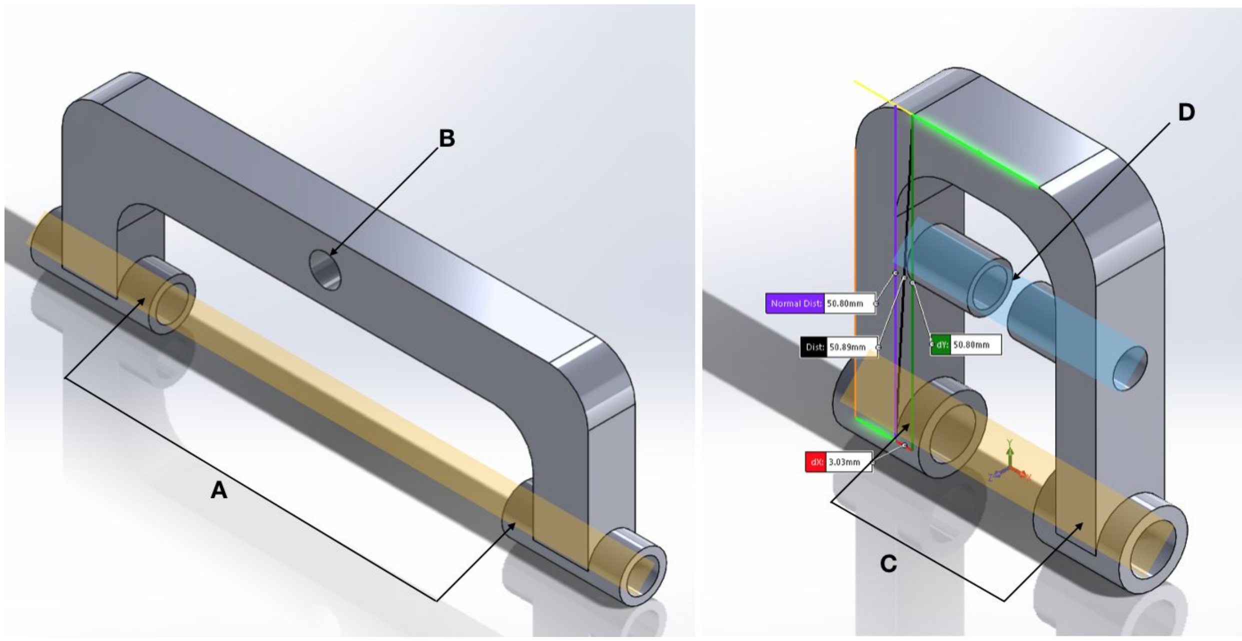

a) Hinge b) Gear Rack Support

Figure 33: First Iteration Center Mechanism

In this iteration, there are two parts in the center mechanism. The horizontal kite pole goes through the orange highlighted sections with a force-fit gear in the center. The second gear is a loose-fit on a quarter inch dowel pin in between section D on the Gear Rack Support. The rack is glued on the Rack Support Pole shown in Figure 32, sitting on the bottom of the “U” shaped Gear Rack Support part. Both section A in the Hinge and section C in Gear Rack support were loose for the eight-millimeters pole to move. The force-fit center gear moves when the rack is pushed, moving the whole horizontal kite pole. By turning the gear and pole, the Ferry Kite’s angle of attack could be adjusted.

The Rack Support Pole is directly attached to Rack Support, which is free to move on the Full Length Pole. When the front of the rack is pushed by a stopper mechanism on the stationary tether, the Rack Support slides with the rack backwards, pushing the gears to turn. The gears then changes the angle of attack of the Ferry Kite.

The Main Support parts are assembled with screen door wheels and they will sit on the stationary tether with low friction. Three Main parts and the Full Length Pole should also balance the Ferry Kite to maintain stability so that the Kite would stay perpendicular to the wind direction and aligned with the stationary kite.

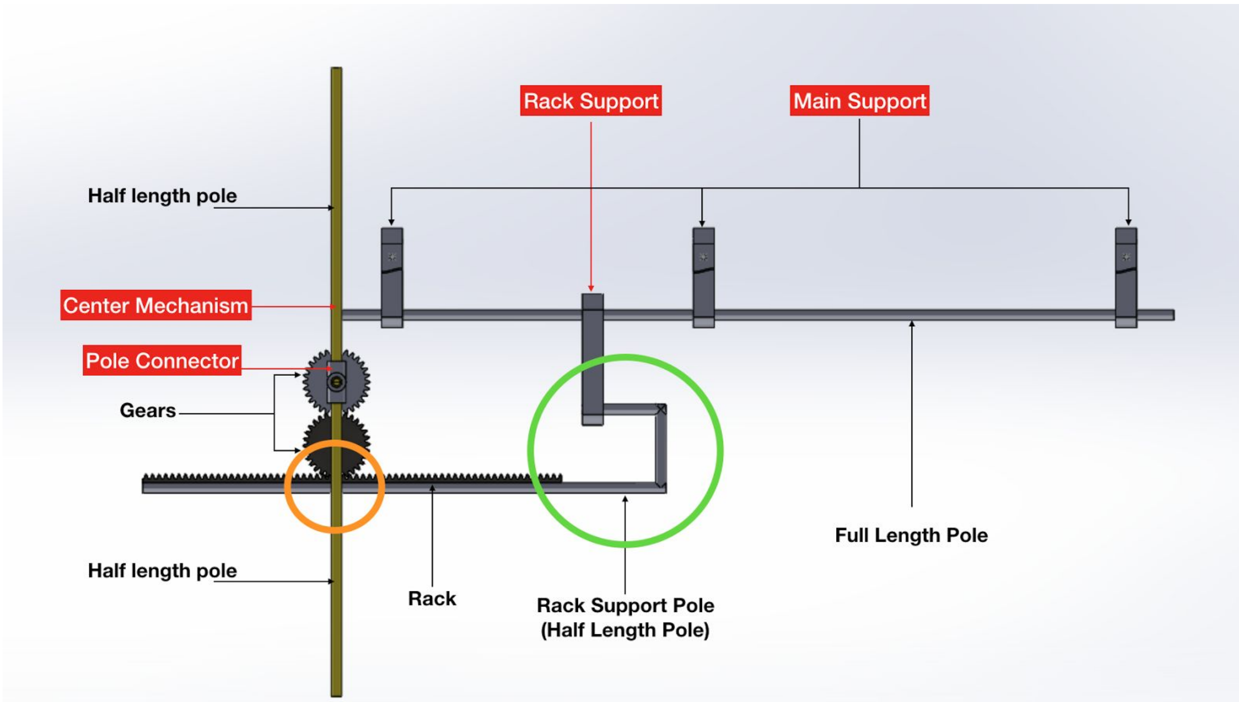

Figure 34: First Iteration Design Side View Highlighting the Problematic Parts in Lab Testing

After the first lab testing, the center mechanism was only functioning when a team member was holding the Gear Rack Support and the Rack Support Pole as highlighted in Figure 34. The long rack and Rack Support Pole was unstable rubbing against the Gear Rack Support. Instead of pushing the rack forwards/backwards, it pushed the Gear Rack Support up without moving the gears. Due to the weight of of the kite itself and the location of the Main Parts, the Ferry Kite was far away from the stationary tether. However, the Full Length Pole and the Main Parts were balancing the system well, but really heavy.

As a result of the first lab testing, the Gear Rack Support and the Hinge were combined to eliminate unnecessary degrees of freedom. It also made sure that the two parts would remain in the same plane. The Full Length Pole was shorten to half its length and pushed forward more so that one of the Main Part could be holding up the system from in front of the Ferry Kite and raise the center mechanism closer to the stationary tether. It was decided that the Ferry Kite only need to turn 90 degrees in angle of attack to be able to accomplish power and retraction phases. Therefore, the distance that the rack need to travel was measured. Electrical tape was used as stoppers and taped on the shortened Full Length Pole to make sure the Ferry Kite would only turn in a controlled manner.

Final Ferry Design

In the final ferry design, the full length poll, the rack support poll and the rack are shortened to further stabilize the ferry kite, reducing the weight of the center mechanism. As shown in figure 35a, the ferry kite is set on the main kite tether on three points. The main parts are assembled with screen door wheels to reduce friction on the line. Rigid plastic parts are designed and fabricated to secure the inner corners of the kite fabric and each plastic part is glued on to the polls to eliminate any unwanted moving. The center mechanism is shown in figure 35b. The rack is reduced to an inch long and glued to the orange poll. The upper gear is glued onto the pole so it is secured in place to allow only rotational freedom with the pole. The bottom gear is supported on each side so it does not slide around, but is free to spin around the pin it is on. The longer main part in front is loosely fitted on the full length poll and tightly fitted on the rack support poll. When the upper stopper on the main tether line hits the front of the main part highlighted in figure 35b, the main part slides on the full length poll that then pushes the rack support poll, turning the gears and the kite fabric in a controlled manner. The rigid stoppers on the full length orange poll will control the rotational degree and ensure the aerodynamic forces on the fabric reduces so that the kite can fall along the main kite tether.

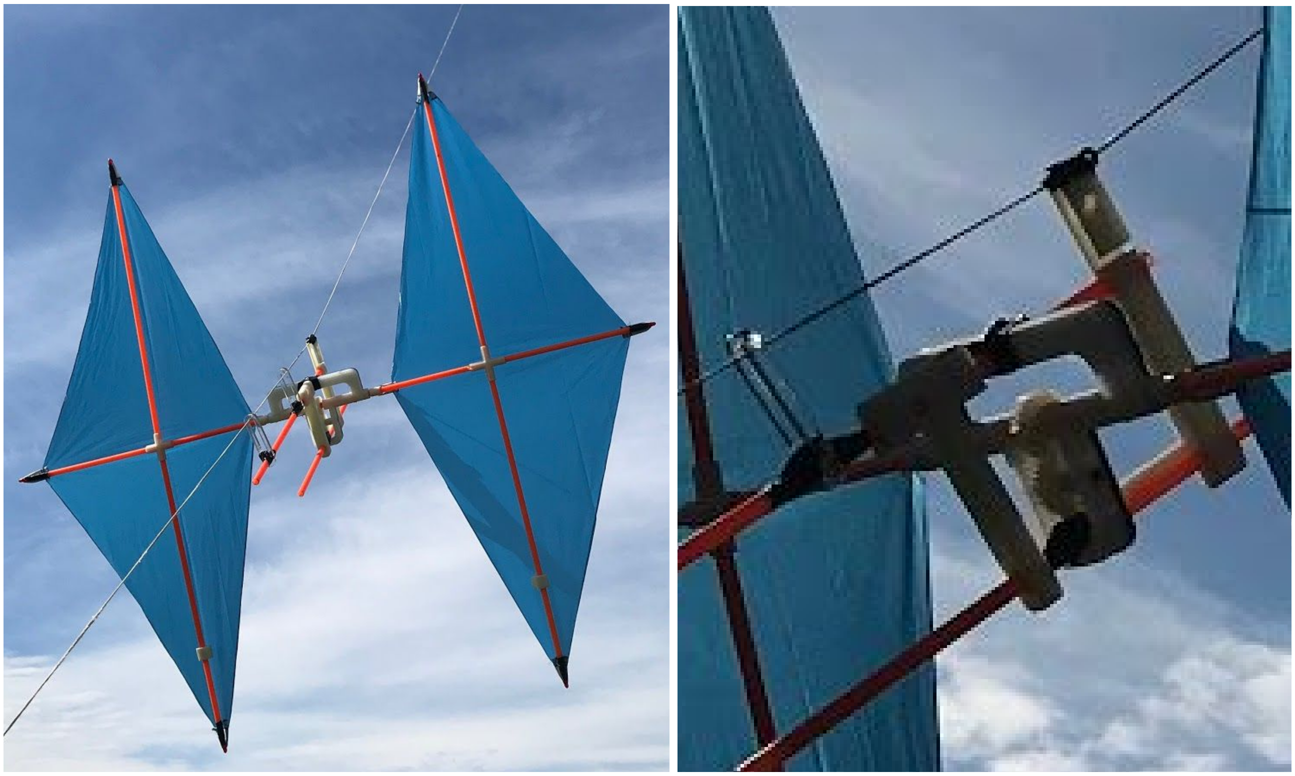

a) b)

Figure 35. Ferry Kite Final Design

Ferry Wing Loading

As was mentioned in the Popper Wing Loading section previously, wing loading measures how much weight is supported by how large of an area. We measure wing loading by dividing the total weight of the kite by its projected area. For the ferry kite, the projected area would just be the area of the kite material since it is flat.

$$Wing\ Loading = \frac{total\ weight}{projected\ area}$$

The dimensions of the ferry kite can be seen in the figure below.

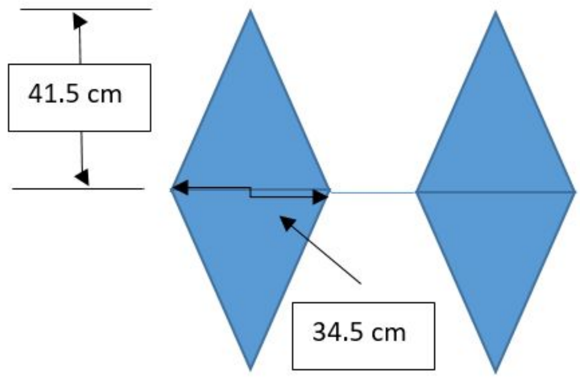

Figure 36. Dimensions of Ferry Kite

The two halves of the ferry kite are identical, and the top and bottom halves are symmetrical. The area of one triangle is as follows:

$$area = (Base * Height)/2$$

The area of one triangle comes out to be 715.875 m^2. The total kite area is as follows:

$$4 * \ 715.875\ cm^2 = 2863.5\ cm^2 = 0.28635\ m^2$$

The mass of the ferry is 292 g which translates to 0.292 kg. This mass can be multiplied by 9.81 m/s^2 to calculate the ferry's weight, which is 2.865 N. The wing loading can then be calculated as 10 N/m^2.

Ferry Testing

Figure 37: Initial Ferry Field Testing

The initial field testing for the updated Ferry Kite design was conducted at Blue Hill Weather Observatory on September 28, 2017. The kite balanced well on the stationary tether and was operating successfully. The tether angle of the stationary kite is really small, but the ferry kite maintained in power phase. However, without any load on the bottom half of the kite, the Ferry Kite was unstable. As the wind pushed the kite along the stationary tether, the kite twisted past its tape stoppers. The Ferry Kite reached the top stopper on the tether within 20 seconds. The tether rope burnt through the first Main Part in front of the kite and created a divot in the third Main Part in the back since the screen door wheels were not installed. The gears were too loose that the kite was being pushed to retraction phase from power phase by wind during the powering phase.

The electrical tape stoppers on the shortened Full Length Pole were replaced by force-fit physical stoppers to avoid unnecessary movements over 90 degrees. The force-fit connectors were glued down to eliminate degrees of freedom. Teflon was used to create more friction between the horizontal pole and the center mechanism in order to address the issue that it was too easy to move. Another extended Main Part was added to the system that the rack could be hold in front of the Ferry Kite as well. The extended Main Part was loose fitted on the shortened Full Length Pole, and tight on the Rack Support Pole. It would push the extended Main Part along the shortened Full Length Pole and push the rack to turn the gears and the kite. This should make it easier to push the rack and ensure that the Ferry Kite would only change its angle of attack when being pushed by the stopper on stationary tether. The Ferry Resetting Process was also implemented and the load on the bottom half of the Ferry Kite would help stabilizing the system during power phase.

Ferry Resetting Process

The Ferry Resetting Process is simpler than the Popper Resetting Process. As shown in figure 36, the Ferry only need to be pulled on two points to be reset to initial power phase condition. Therefore, two physical stoppers were added to the lower Half Length Pole. A rope was tied to the poles and stopped by the stoppers.

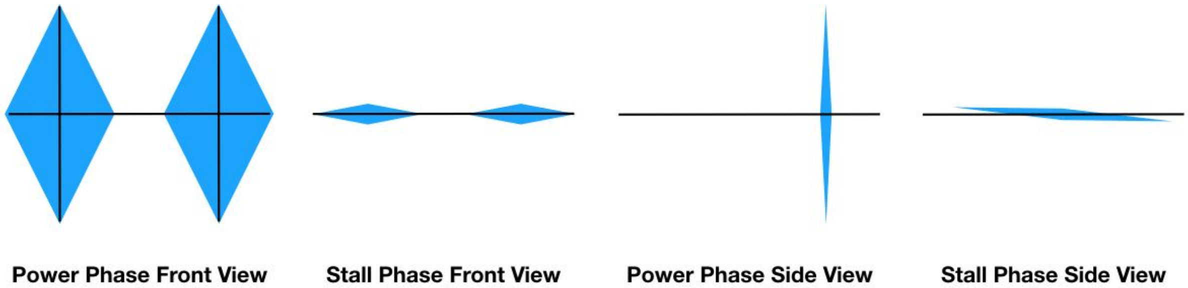

Figure 38: Ferry Two Phases Diagram

Figure 39: Ferry Resetting Process When Ferry is at Higher Stopper Below Main Delta Kite

2.4 Ground Pump Design

Converting the mechanical energy of the kite into the useful transport of water requires not only a working and efficient pump and piping, but also efficient transmission and retraction systems. The testing that these components of the initial prototype from Van Blarcum received, the issues that they faced and some of the solutions to these problems are discussed in detail in this section.

2.4.1 Ground Structure and Power Transmission System

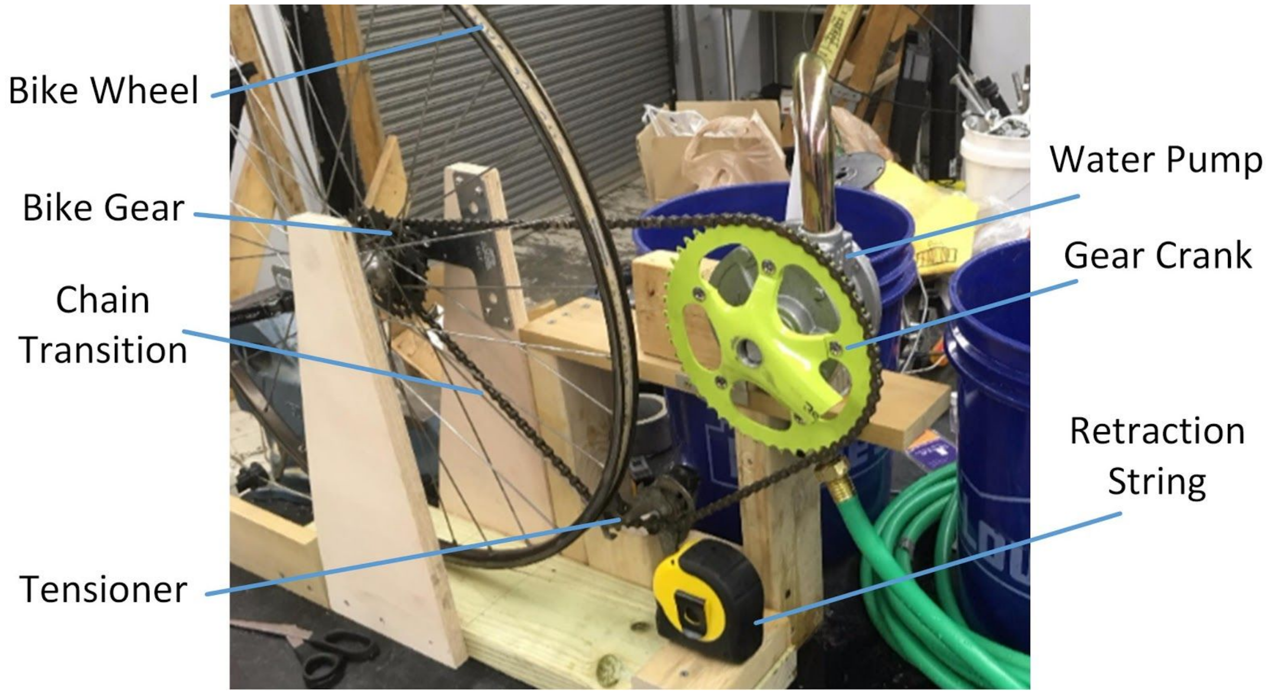

Figure 40. Gear Train from Van Blarcum's (2017) System

In Van Blarcum's (2017) System, the pump was located behind the bike gear. When the wheel is turned, the chain suspended between the pump and the bike gear cannot be sufficiently tensioned. The tensioner was installed upside down between the bike wheel and the water pump which failed to tension the whole chain effectively. Therefore, chain slip happened constantly, and the power transmission lacked stability.

To improve the power transmission efficiency and prevent the chain slip, a new crank with thinner teeth will be necessary, and the location of the pump and the tensioner should be changed. The pump and the pump holder will be taken off and then moved forward and fixed in front of the bike gear. Since the oil pump used in Blarcum's system was changed to a rotary hand pump, more reinforcements such as pump holders will be built to stabilize the pump. The tensioner will be moved closer to the bike gear but not so close that it will interrupt the bike wheel. The alignment among the tensioner, bike gear and the gear crank need to be taken into consideration after placing the pump and tensioner at more suitable places. Based on the specific needs - more torque or more velocity - specific gears on the bike gear and the gear crank need to be chosen. Then the chain will wrap around the tensioner and those chosen gears on the crank and bike gear. To prevent the chain slip, the gears and the tensioner should be on the same plane and keep the alignment during the power generation process.

Figure 41. Standard Bike drivetrain system

The power transmission system would be more similar to the bicycle drivetrain system, and the only difference is that in the ground system, the driven force will be induced from the bike wheel instead of the gear crank. When the ferry kite pulls the ferry kite string, the bike wheel will turn counterclockwise, and therefore, the upper portion of the chain will be tensioned spontaneously and the lower portion of suspended chain will be sufficiently tensioned by the bike tensioner.

Since a bike winch, which adds the gear reduction between the bike wheel and the retraction spring, needs to be added on one side of the bike wheel, one of the frame walls needs to be moved outward to save enough space for the bike winch. The location of the retraction spring will be changed accordingly to align with the bike winch.

2.4.2 String Slip Prevention

One serious problem with the initial prototype was that the string wrapped around the bike wheel was not well secured. The lips along the edges of the wheel were not large enough to effectively contain the string wrapped around it, leading to frequent cases of the string coming off and getting tangled with the rest of the system. Furthermore, the string was not directly attached to the wheel but merely wrapped tightly around it, making motion transfer completely reliant upon unreliable friction.

To prevent this, a series of curved rollers of varied sizes (see figures 42 and 43) were placed around the lower edge of the wheel - where the string was prone to getting loose - such that they pressed against it, ensuring that the string would have no gaps through which to escape and get tangled:

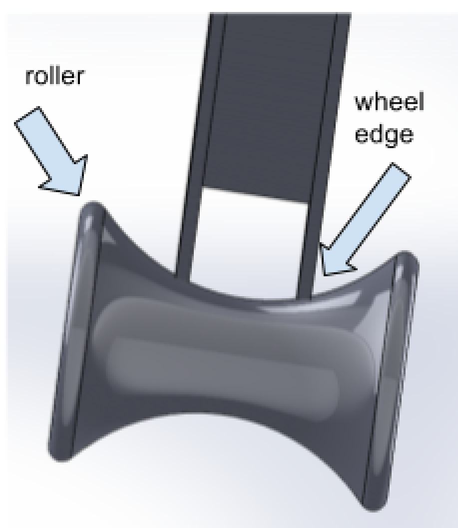

Figure 42. Roller at the edge of the bike wheel.

End diameter: 4.45 cm; Middle diameter: 2.02 cm; Length: 6.35 cm

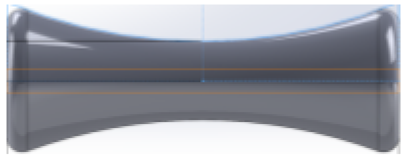

Figure 43. smaller roller.

End diameter: 2.275 cm; Middle diameter: 1.27 cm; Length: 6.35 cm

The purpose of the concave sides of the rollers was to funnel loose string back in-line with the wheel's edge. This shape had the added benefit of making it easier to maintain full contact between the edge of the wheel and the rollers as well. Initially, there was concern that these rollers would add friction to the wheel and reduce efficiency. To test this, the tether wrapped around the wheel was pulled by a fishing scale when only the friction of the wheel and rollers were in effect. This condition was accomplished by detaching the chain connecting the wheel to the pump's gear crank and putting a screwdriver through a loop in the string between the bike winch and the retraction spring to prevent full retraction:

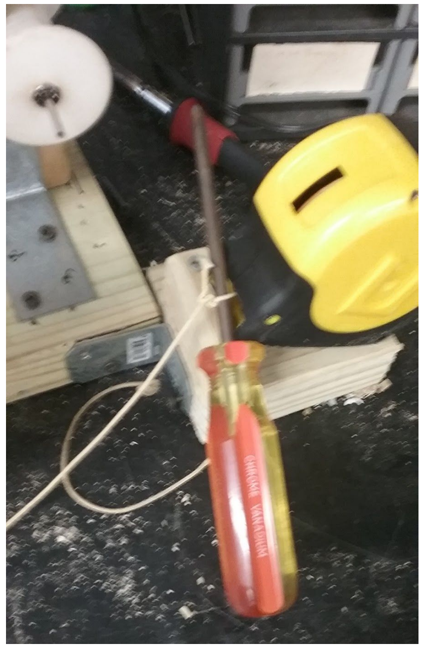

Figure 44. Intentional, reversible jamming of the retraction system with a screwdriver.

Next, the wheel was turned backwards a certain amount to create slack in the retraction system, leaving room for rotation that was unimpeded besides the internal friction of the wheel and rollers.

Another solution implemented was the following “two-string” system:

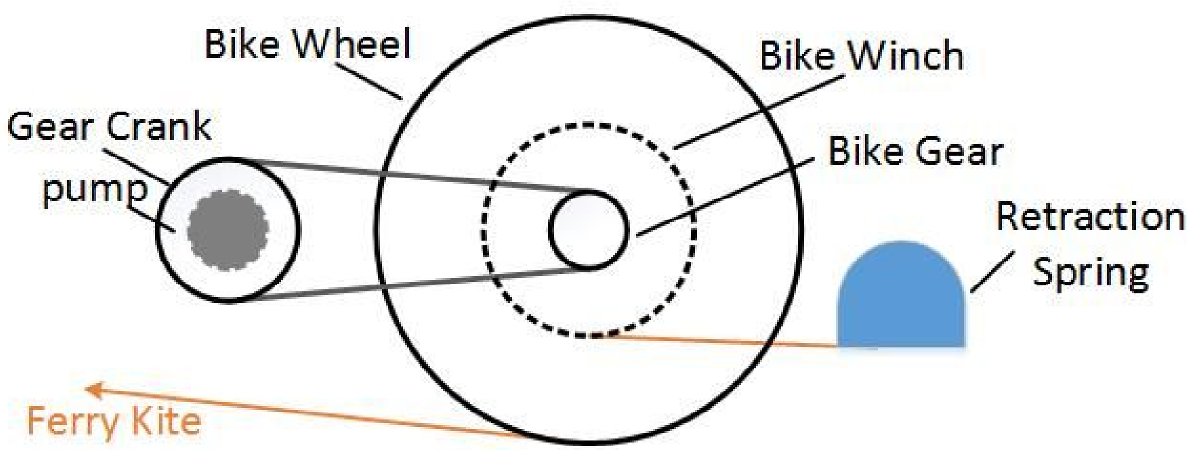

Figure 45. Two-string system. In this setup the retraction string leading to the retraction spring pulls on the bike winch to retract the popper which is pulling on and held by the kite tether.

The primary advantage of this system was that it transferred energy from the kite to the wheel via tension, making it more reliable than the original configuration which relied solely on friction. Another advantage of this system was that the length of string connecting the wheel to the kite rubbed against the length connecting the wheel to the retraction system with the original configuration while they remained separate with this two-string configuration - improving efficiency.

The challenge with implementing this change was having to not only construct the bike winch, but effectively secure it to the bike wheel. This was accomplished using a set of clamps and 8 nuts and bolts - see figure 61 in section 3.

2.4.3 Retraction Force Reduction

Another significant problem with the prototype was that the retraction spring - provided by a repurposed tape measure - exerted too much force on the kite as it flew out. Due to the spring's constant and stretch range, the hopper could not fly out to its intended distance under reasonable wind conditions as the retraction force increased too much by then.

One solution was the following configuration:

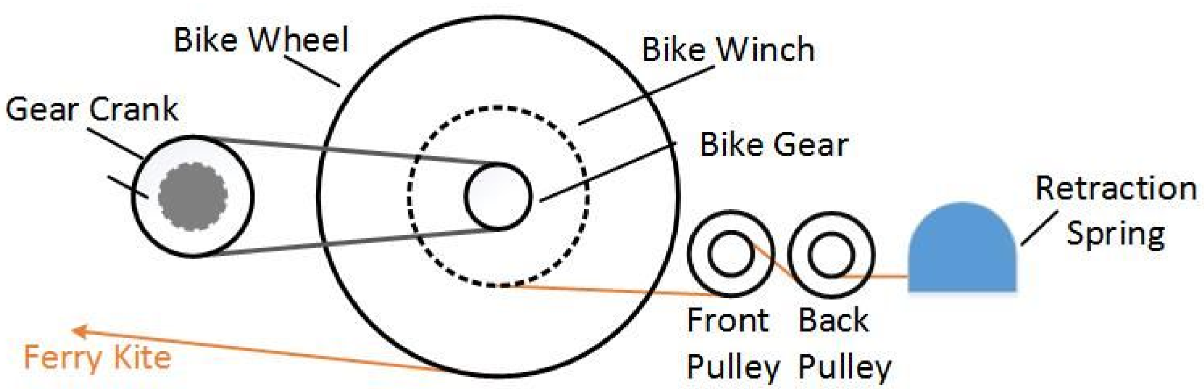

Figure 46. Spring-based retraction system with pulleys.

This configuration used a series of pulleys between the bike winch and retraction spring and the ratio between the bike winch's and bike wheel's diameters to reduce the retraction force experienced by the kite while increasing the distance to which it could fly. To compensate for the reductions in the system and subject the kite to sufficient retraction forces, the spring was simply stretched a certain distance before being connected to the back pulley roller. A stopper was also added to keep the kite from retracting too far. This way, the minimum retraction force provided by the spring would always be sufficient regardless of the kite's position in its flight. The variation in retraction force that was previously encountered would be minimal as - thanks to the reduction ratios of the system - the kite's trip upward would translate to little additional stretching in the spring and what little increase in the spring's force would occur would be reduced several-fold. One potential problem of this setup was the possibility that the pulleys would reduce the retraction force too much and not allow the kite to fully retract even if the spring was given a minimum stretch. Other issues that remained were gradual - and slow - degradation of the spring with use and increased mechanical complexity. These problems were deemed acceptable costs for making a compact, portable and efficient system. Like with the rollers used to keep the string on the wheel, any added friction was reduced using ball bearings.

Pump Torque

The ground system can be divided into three main parts - the bike wheel part, the pulley-spring part, and the pump part. Assume all the components in the system are in equilibrium. When the popper is climbing up, it will drive the bike wheel. Due to conservation of energy, the input power should be equal to the power output.

$$P_1 = P_2 \quad [14]$$

Which can be written as

$$F_1 r_1 \omega_1 = F_2 r_2 \omega_2 \qquad [15]$$

Since the bike winch, the bike gear, and the bike wheel are concentric and attached together, the angular velocity of each component is the same. Therefore, the equation can be simplified to

$$\omega_1 = \omega_2 \qquad [16]$$

$$F_1 r_1 = F_2 r_2 \qquad [17]$$

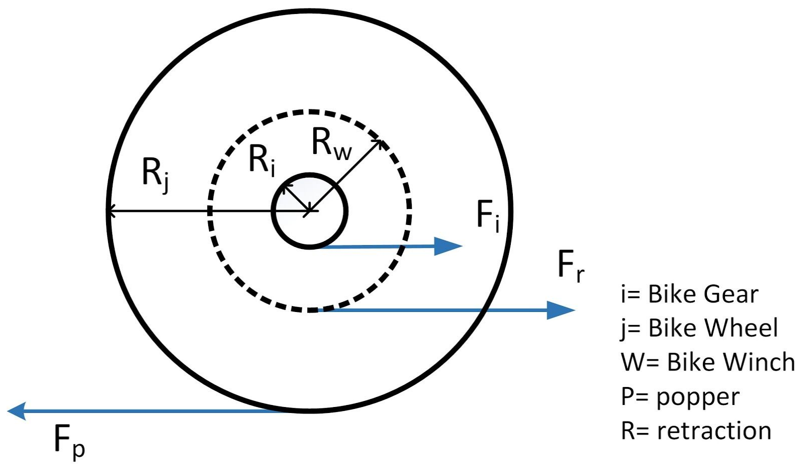

Figure 47. Force diagram of the bike wheel system

In this case, for the bike wheel part, assume the system is in equilibrium, the equation can be written as

$$F_p R_j = F_r R_w + F_i R_i \qquad [18]$$

Since the number of pulleys (n) are not confirmed, according to reduction ratio (2.7:1) for each pulley, the spring force equation can be written as

$$F = (\tfrac{1}{2.7})^n k * l \qquad [19]$$

the equation for the bike wheel can be changed to

$$F_p R_j = (\tfrac{1}{2.7})^n kl * R_w + F_i R_i \qquad [20]$$

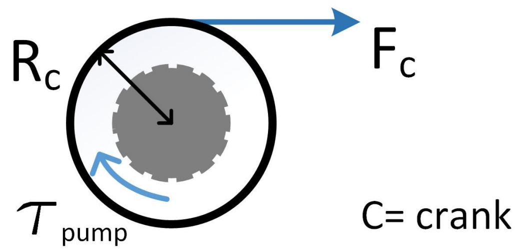

Figure 48. Force diagram of the pump and crank system

In this ground system, the bike wheel part is connected to the pump part by a chain. Therefore, the force acting on the bike gear will be transmitted directly to the gear crank attached on the pump, which means the two forces have the same magnitude.

$$F_c = F_i \quad [21]$$

Based on the equation 17, when the crank and the crank gear are concentric and connected tightly together, the torque input is equal to the torque output. As a result, according to equations 19 and 21, the torque the pump receives is equal to

$$\tau_{pump} = F_c R_c = R_c (R_j F_p - (\tfrac{1}{2.7})^n k l R_w)/R_i \quad [22]$$

Pump Angular Velocity

According to equation 16 and the angular velocity to linear velocity equation

$$v = \omega * R \quad [23]$$

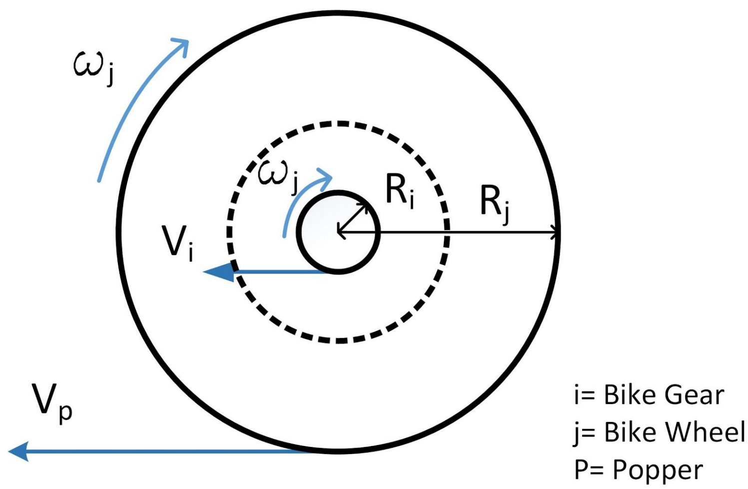

Figure 49. Velocity of each components in the bike wheel system

when the bike gear is at the center of the bike wheel, the linear velocity at the edge of the bike gear, which connected to the gear crank by the chain, is equal to

$$V_i = \frac{V_p}{R_j} * R_i \qquad [24]$$

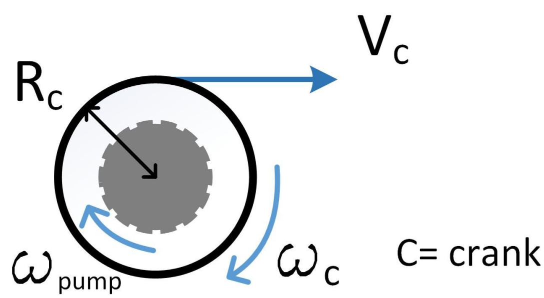

Figure 50. Velocity of pump and gear cranks

Assume the chain connected between the bike gear and the crank gear is tight and efficient enough to drive the crank gear at the same speed as the bike gear. Therefore, the linear velocity of the two parts should be the same and use the relation provided in equation 23, the angular velocity of the pump is

$$\omega_{pump} = V_p * \frac{R_i}{R_j R_c} \qquad [25]$$

Torque and Angular Velocity Calculation

According to equation 22 and 25, the torque and the angular velocity can not be maximized at the same time. Therefore, different sets of gears will be used in order to get the largest torque or highest angular velocity.

From the in lab measurement, the spring constant of the retraction spring is around 2.2304 N/m; the radius of the bike wheel is 0.312m; the radius of the bike winch is one third the radius of the bike wheel, 0.104m; the radius of the bike gear can be 0.0598m, 0.0518m, 0.0379m, 0.0339m and 0.02991m; the radius of the gear crank can be 0.08375m and 0.10768m.

To maximize the torque act on the pump, the smallest bike gear (0.02991 m) and the larger crank gear (0.10768 m) will be used. Based on the results from the air team calculation, force produced by the ferry ite varies from 1.32 to 26.37N, so two expressions to express the pump torque according to different Ferry kite forces are

$$\tau_{pump} = 0.10768/0.02991 * (0.312 * 1.32 - 2.2304 * L_{string} * 0.104) \quad (F_{ferry} = 1.32\ N)$$

$$\tau_{pump} = 0.10768/0.02991 * (0.312 * 26.37 - 2.2304 * L_{string} * 0.104) \quad (F_{ferry} = 26.37\ N)$$

Assume the retraction spring will be pulled out for 0 to 5 meters due to the reduction ratio, and base on these two expressions, the relationship between the output torque and the string length can be shown in Figure 51and 52 with different gear ratios.

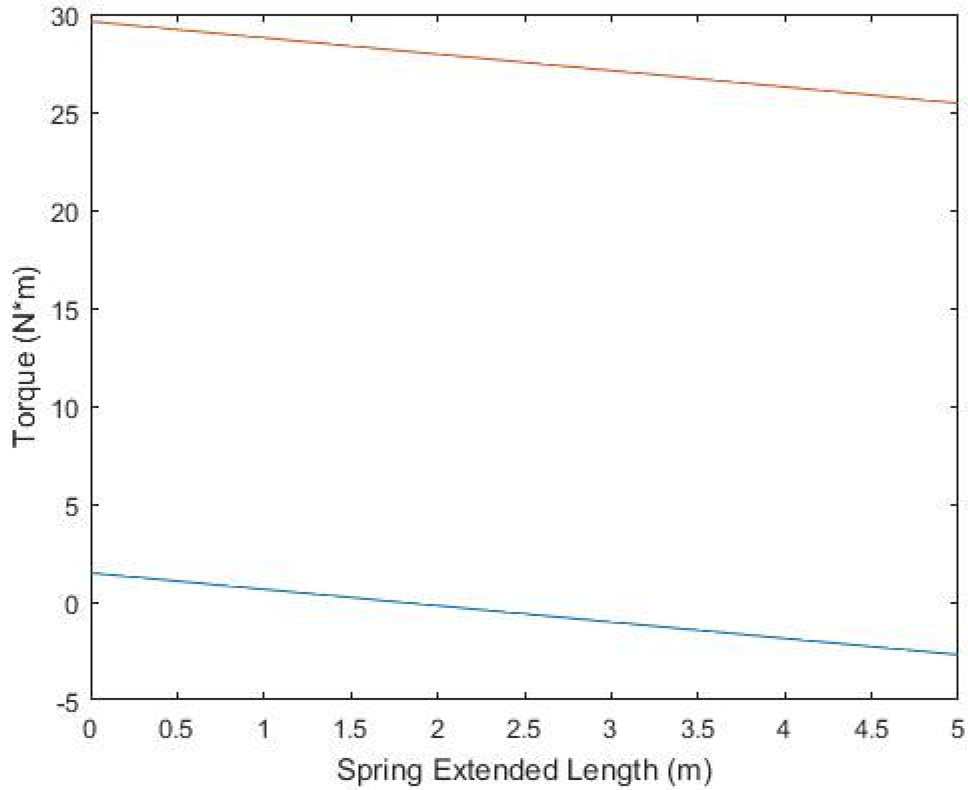

Figure 51. Torque in relation to spring extended length with maximum torque gear ratio. The red line represents the torque and length relation when the force from the ferry is 26.37N; The blue line represents the relation when the ferry force equals 1.32 N.

To get the minimum torque output and maximize the pump angular velocity, the largest bike gear (0.05982 m) and the smaller crank gear (0.08375 m) will be used, and the expressions are

$$\tau_{pump} = 0.08375/0.05982 * (0.312 * 1.32 - 2.2304 * L_{string} * 0.104) \quad (F_{ferry} = 1.32\ N)$$

$$\tau_{pump} = 0.08375/0.05982 * (0.312 * 26.37 - 2.2304 * L_{string} * 0.104) \quad (F_{ferry} = 26.37\ N)$$

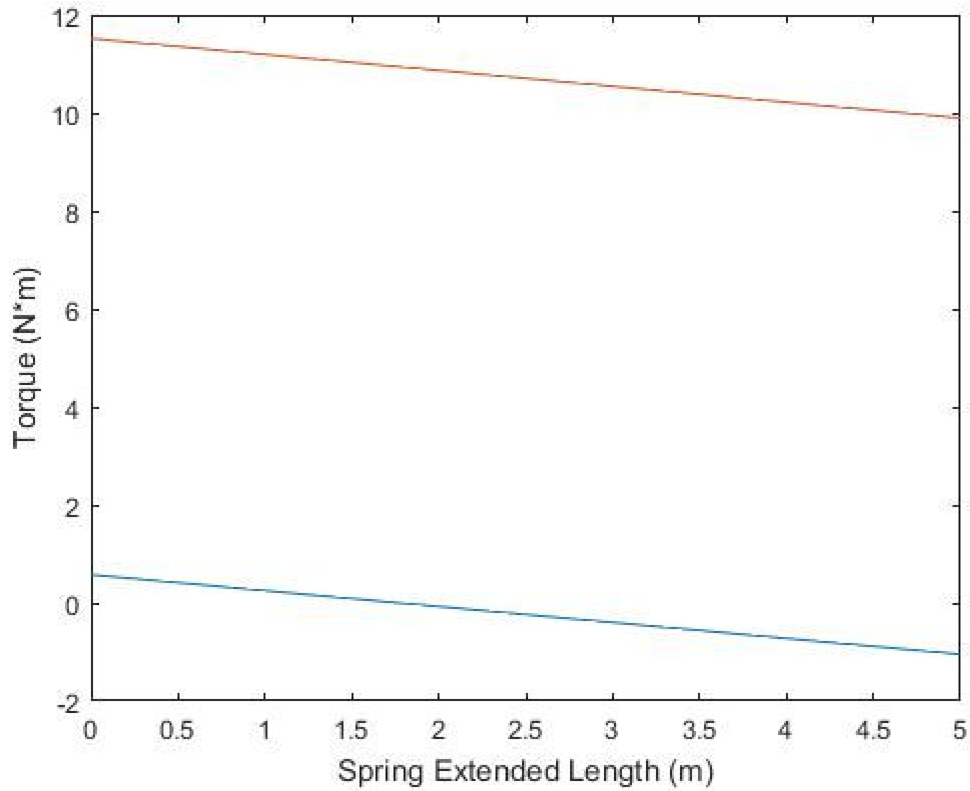

Figure 52. Torque in relation to spring extended length with maximum angular velocity gear ratio. The red line represents the torque and length relation when the force from the ferry is 26.37N; The blue line represents the relation when the ferry force equals 1.32 N.

Assume the the velocity of the ferry kite is constant and equal to 1 m/s, based on the the measurements the maximum pump angular velocity equals 2.2893 rad/sec when using the smallest gear on the gear crank and the largest gear on the bike gear; the minimum pump angular velocity equals 0.8903 rad/sec while using the largest gear on the gear crank and the smallest gear on the bike gear.

2.4.4 Pump and the Priming System

The rotary pump needs to be primed before being turned in order to extend the pump's life. The priming system is designed to be connected to the inlet of the pump. The system includes a Tee connector, an elbow connector, two reduction adapters, one pvc to brass adaptor, a seal cap, a hose, and a directional valve.

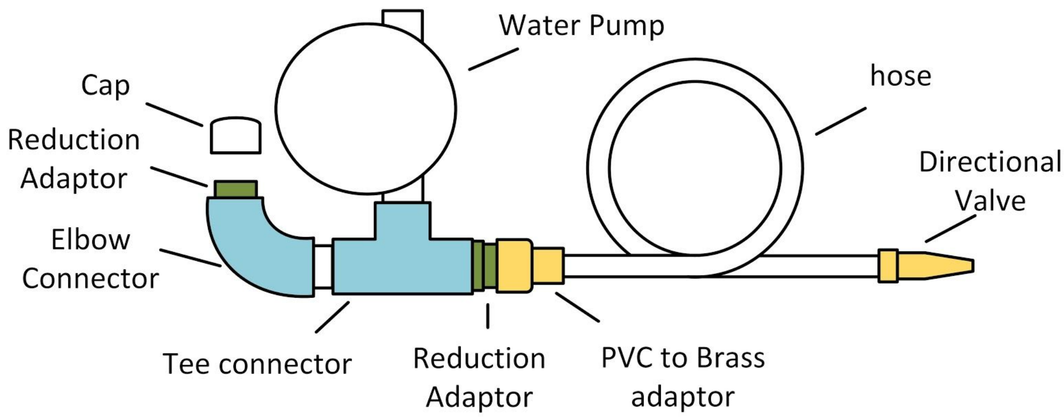

Figure 53. Priming system schematic view

The sealing condition and the performance of the pump will both be tested in the lab. To prepare the lab test, the directional valve would be placed in the bucket, and the water will fill the hose from the elbow. When the water level is 1 centimeter below the open end of the elbow connector, the water should stop being added, and the cap should be screwed to seal the system. In the lab test, the wheel will be turned manually and drive the water pump at constant velocity. The change in water level will be recorded to qualify the sealing condition, and the volume of water that comes out will be used to determine the pump performance.

To test the torque necessary to drive the pump, the pump's intake was set into a bucket of water and a beaker was set below its output nozzle. Next - and before every test - the pump's crank was rotated until water came through to lubricate the pump and simulate the load of the water when used in the field. The crank handle was then positioned so that its proper rotation direction for pumping would bring it downward and a second bucket was hung over it by the handle. For each test, water was slowly poured into the second bucket until its weight pulled down on the crank and rotated it. This bucket was then weighed and the recorded weight was multiplied by the distance between the crank's grip where the bucket was hung and the center of the crank to get the minimum necessary torque. The bucket was then emptied and the test repeated several times to get a reliable average.

3 RESULTS

3.1 Aerodynamic Team

Final Popper Testing

In the end, the new popper kite design had some deficiencies. The third iteration of the popper design was promising, but since the popping mechanism broke, we were unable to proceed with the design. The breaking of the popping mechanism raised a large concern as to why the popping mechanism broke. We had only field tested with it a handful of times. It appears that the forces created with the larger kite surface area may have been too powerful for the mechanism to handle.

Final Ferry Testing

Our final field testing took place on October 11th, 2017 at Moore State Park in Paxton, MA. The wind conditions were 11 km/hour blowing from East to West. For our first attempt, we left electrical tape on the main parts where the ferry would slide on the stationary tether. This can be seen in figure 54. We did this since our final 3D printed parts for the main parts was not printed yet. The electrical tape prevented the stationary tether from burning through the plastic.

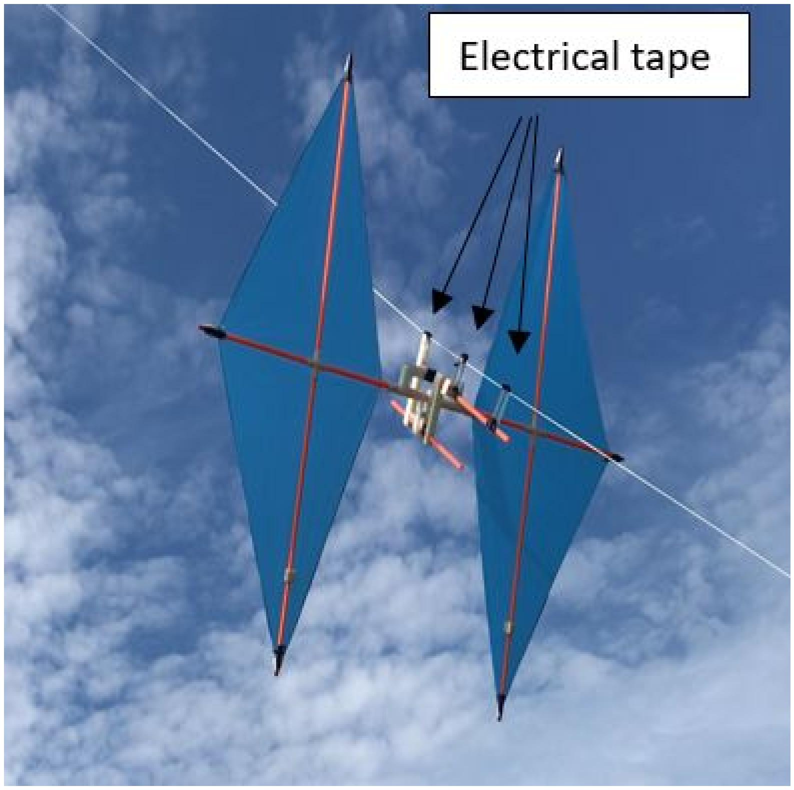

Figure 54. Ferry Kite with Electrical Tape on All Main Parts

For this first attempt, one of the team members held onto the ferry kite tether to simulate resistance from the pump. This resistance will help keep the ferry in the power position as it goes through the power phase.

The ferry was slow to go up the line at first. The ferry reached the top in roughly 47 seconds. This is much slower than when the ferry went up the stationary tether during initial ferry testing at Blue Hill Observatory. This is due to the electrical tape we added to protect the acrylic pieces that we mentioned above. The electrical tape added a significant amount of friction and thus slowed the ferry down.

For the second attempt, we took off the electric tape from the last two main parts on the ferry, so only the very front main part would have the tape. This can be seen in figure 55. The reduction in friction significantly increased the speed of the ferry. It reached the top in roughly 25 seconds.

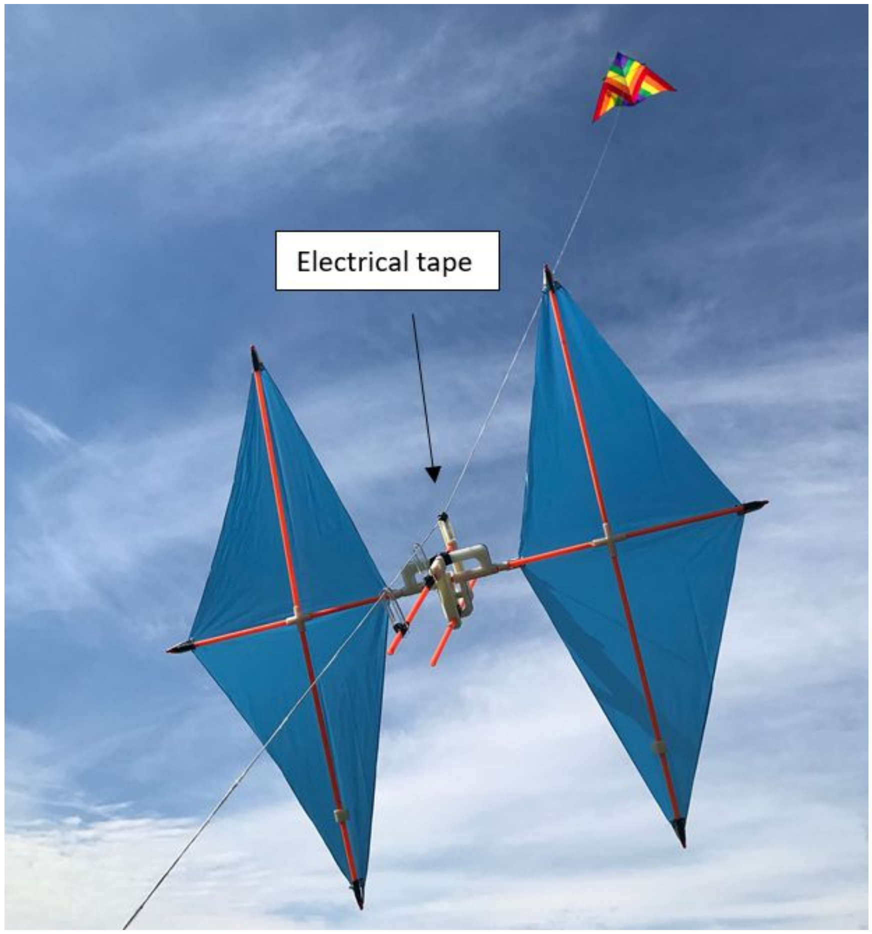

Figure 55. Ferry Kite with Electrical Tape on Front Main Part

During both attempts, the ferry stayed in the correct position throughout the power phase. The kite was not flipping around in the wind and balanced itself on the stationary tether correctly. However, when the ferry hit the nut at the top of the stationary tether, it did not turn into the proper stall position. It appears that the wind on the kite was too strong and that the nut at the top of the stationary tether needs to be pushed from beneath the main pole in order to push the rack back. Currently, the nut is only able to push from the top of the main pole.

3.2 Ground Pump Team

Redesigned Ground System and Power Transmission System

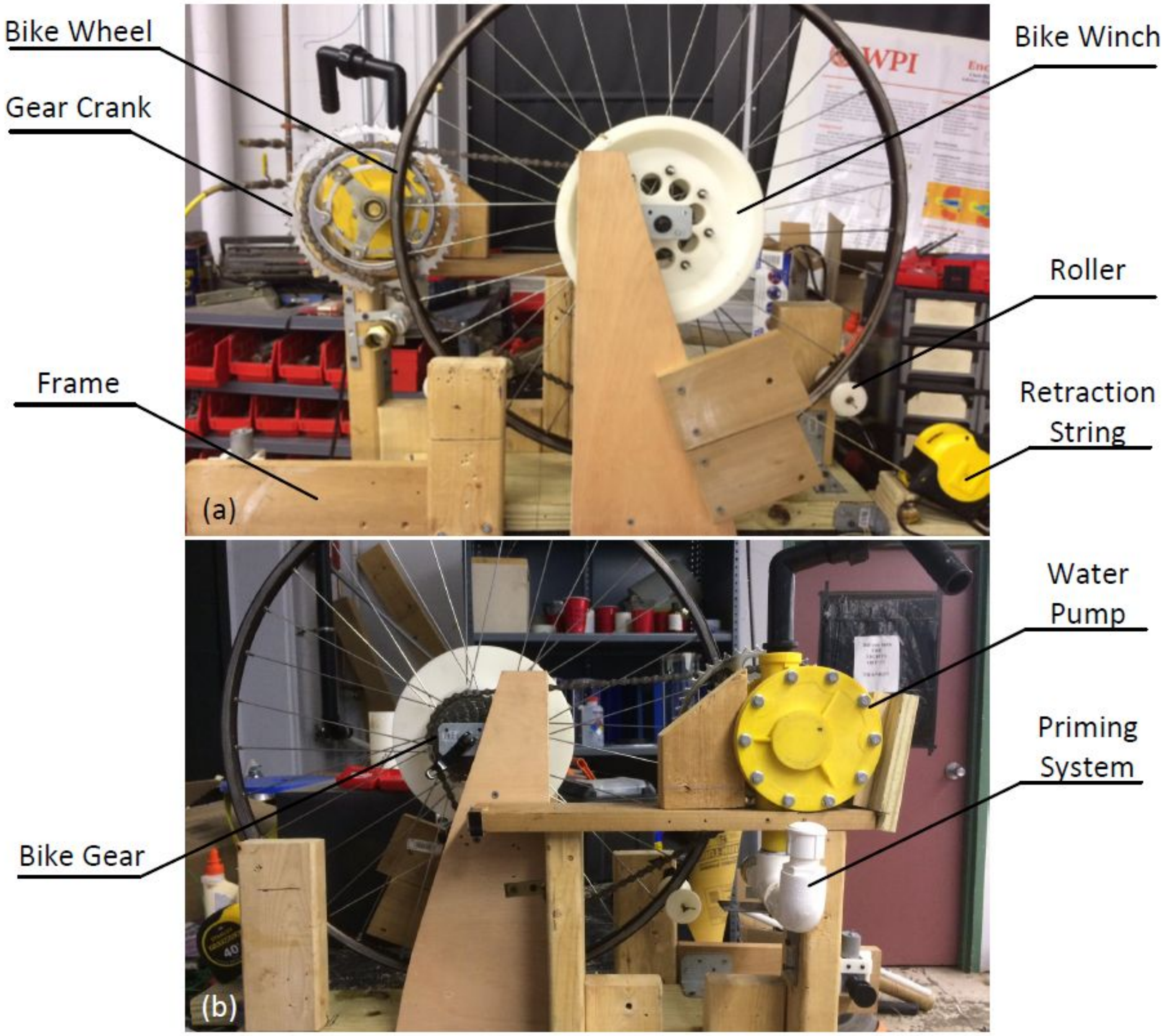

Figure 56. Front View (a) and Back View (b) of the Redesigned Ground System

In the redesigned ground system, the overall size of the setup was not changed too much compared with Blarcum's model. The pump was moved forward and two blocks were used to stabilize the the water pump. The trapezoidal wall further from the water pump was moved outward 4 centimeters to leave more space for the bike winch. The position of the retraction spring was changed so that it would be able to align with the bike winch. Two 1 centimeter wooden blocks were added to create a slope for the retraction spring to prevent the friction between the tether and the upper edge of the it.

Figure 57. Gear Train

The tensioner was installed right below the bike gear. One wooden block was added to elevate the tensioner to the right height so it would be able to align with both the gear crank and the bike gear. After changing the gear crank and relocating the bike tensioner, the chain could be sufficiently tensioned during the power phase and would seldom slip from the crank gear.

For the power transmission system, the smaller gear on the crank and the largest gear on the bike gear were chosen to use in the system since the water pump needs around 4N*m of torque to make it turn, and the average of the pump torque while using the gear combination is more than the necessary torque. Moreover, most pumps need to be turned at a minimum velocity in order to make sure they can work properly. Therefore, the angular velocity became the biggest concern and the gear set with the smaller crank gear and the largest bike gear was chosen.

Rollers and Retraction

Unfortunately, the pulleys not only proved difficult to properly position and secure but also reduced the retraction force to the point where it could not overcome the friction within the system. As such, the pulleys ended up being removed with the entire gear reduction being provided by the 3:1 diameter ratio between the wheel and the bike winch.

In the final design a series of three curved rollers of two different sizes (see figures 58 and 59) are positioned around the lower edge of the wheel such that they press firmly against it. This, in combination with the concave sides of the rollers ensures that there is constant, full contact between them and the wheel's edge, leaving the string with no gaps through which to escape:

Figure 58. Roller at the edge of the bike wheel.

Figure 59. Smaller roller.

The other purpose of the concave sides of the rollers is to funnel string back in-line with the wheel's edge as it goes slack. Pulling on the kite tether wrapped around the wheel and then releasing it to be pulled back in by the retraction system rarely if ever resulted in the string coming loose and tangling. There was, however, one roller towards the back which did not maintain full contact with the wheel and gave the string slightly more room to come loose.

Any additional friction that was once worried to have been created by the rollers is minimal thanks to the incorporation of small ball bearings at their ends. Pulling on the tether wrapped around the wheel only requires 1 to 2 newtons of force to turn it when only the friction of the wheel and rollers is in effect.

Another feature that helps is the “two-string” system:

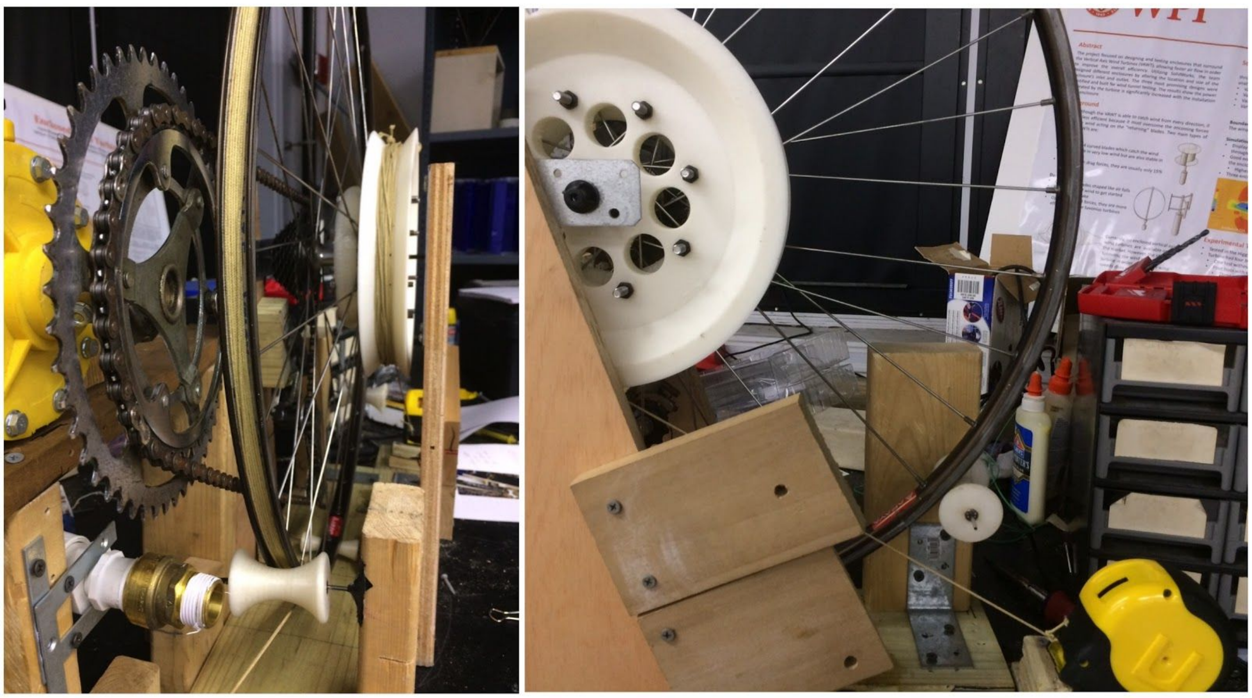

(a) (b)

Figure 60. Two-string system. In this setup the retraction string leading to the retraction spring (b) pulls on the bike winch to retract the popper which is pulling on and held by the kite tether (a).

The primary advantage of this system is that it transfers energy from the kite to the wheel via tension, making it more reliable than the original configuration which relied solely on friction and allowed occasional slip to occur. When the kite tether of the original prototype was pulled - either by the popper or by a team member - the static friction between the wheel and the tether wrapped around it would occasionally give way and allow the wheel to lag behind a bit. This lag was nonexistent with the new tension-reliant system.

Another advantage of this setup is that the length of string connecting the wheel to the kite is kept separate from the length connecting the wheel to the retraction spring. In the original prototype, there was only one string connecting the kite directly to the retraction system. The section of string coiled around the wheel in the middle would rub against itself while being pulled, resulting in potentially energy-wasting friction. With the new system, the two sections of string do not rub against themselves or each other, eliminating the mentioned friction.

Lastly, with a radius roughly equal to one third of the bike wheel's, the bike winch reduced the maximum retraction force experienced by the kite by a factor of three while increasing by the same factor the maximum possible flight range of the kite within the limits of the spring's stretching range. With the minimum retraction force applied that was necessary to overcome friction and allow full retraction, it took 3 to 5 newtons of force to pull out the kite tether around the wheel without the bike chain connecting the wheel to the pump and roughly 10 newtons with the pump connected by the chain and offering additional resistance.

The bike winch is secured to the wheel using the following clamp with 8 bolts and nuts:

(a) (b) (c)

Figure 61. The front face (a) and clamped back side (b and c) of the bike winch.

The ring-shaped clamp consists of four of the following piece held together by the bolts:

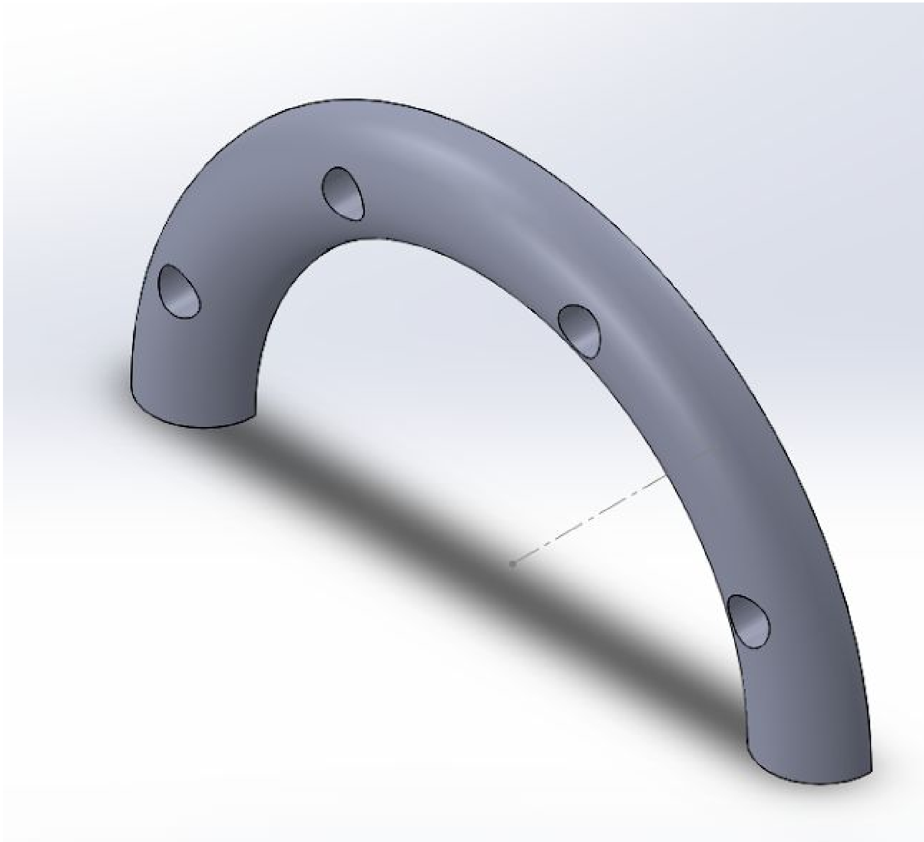

Figure 62. Two of this piece formed a ring and two of those rings placed back-to-back formed the clamp.

Both the winch and the four clamp pieces (see figure 62) were modeled using SolidWorks CAD software and 3D printed separately.

Another important issue to bring up is that the retraction spring was prone to getting stuck in the middle of retraction during the previously mentioned tests. While it could usually get unstuck with a short and quick tug of either string, the issue did make the machine less efficient and more tedious to work with. This seemed at least partly due to the retraction string pressing against the upper edge of the mouth of the retraction spring and creating friction as a result of the retraction spring being tilted lower than necessary to line up with the edge of the bike winch. Mostly though, the issue seemed to come from jamming inside of the retraction spring as the string wouldn’t always retract normally even if it was pressed down slightly or given slack so that it wasn’t rubbing against the mouth of the retraction spring.

Priming system

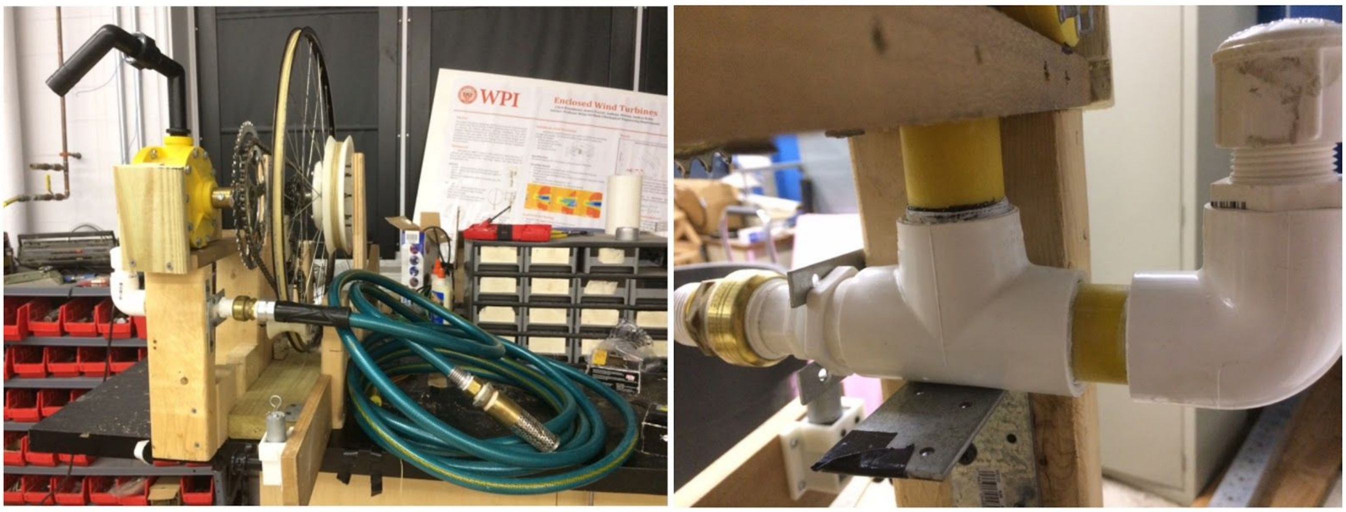

Figure 63. Priming System Piping

In the final priming system, the yellow pipes that came with the water pump were cut into 8 centimeter long segments and served as the connection part between the tee connector and the elbow connector. Seal tape and duct tape were used at the same time to enhance the connection stability and the sealing.

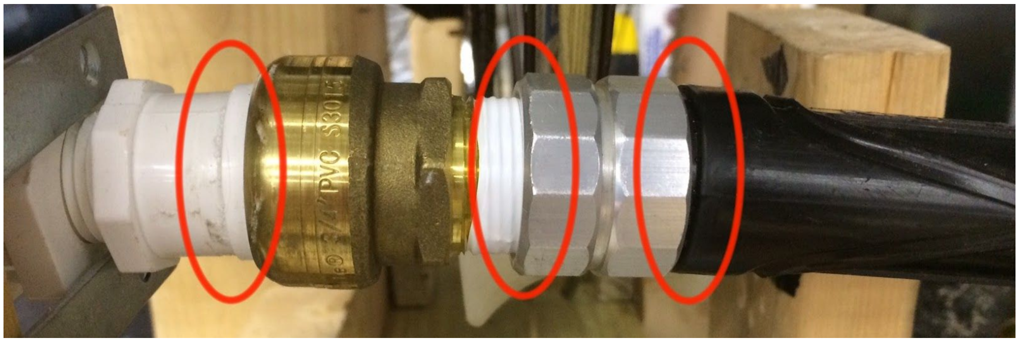

Figure 64. Leaking Spots in Piping System

In the priming test, the wheel was turned at 0.5 m/s to drive the pump. However, the pump failed to pump water out, and minor leaks occurred at one end of the hose, the junction between the hose and the pvc to brass adaptor, and the junction between the pvc to brass adaptor and reduction adaptor. The water level after the test dropped around 1 cm compared with the water level before the testing.

4 RECOMMENDATIONS & CONCLUSIONS

4.1 Aerodynamic Team

Popper

In the future, it would seem that a new popping mechanism would need to be designed in order to withstand the larger wind forces of an increased popper projected area. Ideally, if a popper kite design is going to be pursued further, the popper kite needs to be built from scratch so that all pieces are meant to fit together. For our project, this seemed to be the easier path of the two kite designs, popper and ferry. Instead, a lot of time was used up trying to build off of the original popper.

A future popper design needs to reevaluate how big and strong the popping mechanism needs to be, how to best tension and support a larger surface area popper, and what a balanced resetting mechanism looks like. The current resetting mechanism could be continually used by replacing the copper wires with steel or some other more stable material.

The current popper system is using a heavier pound string than the stationary tether for the delta kite. When redesigning the popper system, a lighter string needs to be implemented so that the popper tether would not cut through the delta kite tether during flight.

Ferry

The ferry mechanism is relatively more reliable than the popper system and the team accomplished the goal of designing a system to replace the popper. It is designed to change its angle of attack, reducing the aerodynamic forces and falls down the main kite tether in a controlled manner. This controlled descent is an important new feature since lack of control of stalled kites during retraction phase was a serious problem with early designs. However, the power phase to retraction phase transition process could be improved more. An elastic band could be used to attach to the the tops of the Ferry Kite and the back of the main pole. It would help to snap the kite back into stall position when ferry reaches the stop below the main delta kite. A locking mechanism may also be added to lock the ferry into position during the power phase, and possibly during the retraction phase. After more testing on the center mechanism to achieve a smooth transition and resetting process, the projected kite area could be gradually increased, recommending starting with bigger diamond shapes to ensure a balanced system. The upper stopper knot on the stationary tether needs to be improved, considering it could be easily attach and easily to take off. Make sure the main parts do not have significant amount of friction when sliding on the stationary tether. Test different types of screen door wheels if possible.

4.2 Ground Pump Team

Unfortunately, due to time constraints and weather conditions the final design could not be field tested with the final modifications discussed in the past two sections. Instead, the ground system ended up having to be tested separately from the air system. Furthermore, some parts of it like the pump and priming system did not have time to be fixed when they were found not to function properly. That being said, a few useful modifications were developed like the concave rollers around the bottom of the wheel while less practical ones were rooted out like the pulley system.

Rollers

As mentioned, the rollers helped significantly in preventing the kite tether from coming loose while adding minimal friction. However, further friction reduction in the wheel and rollers would be helpful in improving efficiency nonetheless. As an extra layer of safety, repositioning the previously mentioned back roller such that it maintains full contact with the wheel could improve the system's resistance to failure by the string coming loose.

Retraction System

It is highly recommended that future iterations of this project use a stronger retraction spring that is more rugged and reliable than a repurposed tape measure. Not only is repurposing the retraction spring a tedious task, it is prone to at least some internal jamming. Furthermore, a stronger spring could offer sufficient retraction forces even with a greater reduction ratio between the spring and the wheel which could result in a more consistent retraction force. It is also recommended that future teams take the time to make sure the source of the retraction force is angled such that the retraction string doesn't rub against any edges - if there are any - on the spring's housing in order to reduce friction.

Water Pump

There are several possibilities about why the water pump failed to pump water. One is that the driven velocity was not enough. Since water pumps always need a minimum velocity to make them able to pump water out, it was possible that during the lab test the velocity given to the pump did not reach the lower limit so the pump was not able to work. The second possibility is that the water pump was damaged previously due to the insufficient priming. In previous field tests and lab tests, the pump was turned without water inside and the lack of lubricant makes the components inside the water pump rubbing against each other cause damage to the water pump. Since the junction between the pump handle and the water pump was removed, the second possibility is not able to be proved. Therefore, finding a more suitable pump might be helpful to improving the performance of the whole system. The commercially available crank EZ Pump is one possible pump to consider in the future design.

REFERENCES

Abramowski, Jasper, and Rolf Posorski. “Wind Energy for Developing Countries.” DEWI Magazin Nr., 16 Feb. 2000, www.dewi.de/dewi/fileadmin/pdf/publications/Magazin_16/06.pdf.

Alex, Lauren, et al. Design of a Data Acquisition System for a Kite Power Demonstrator. Diss. WORCESTER POLYTECHNIC INSTITUTE, 2009.

Allen, D. C., Macalady, A. K., Chenchouni, H., Bachelet, D., McDowell, N., Vennetier, M., ... Cobb, N. (2010, February 5). A global overview of drought and heat-induced tree mortality reveals emerging climate change risks for forests. *Forest Ecology and Management, 259,* 660-684. https://doi.org/10.1016/j.foreco.2009.09.001

Altaeros Energies. (n.d.). *Altaeros energies high altitude wind turbine deploys at 1,000 feet above ground.* [Cropped CGI]. From https://www.designboom.com/technology/altaeros-energies-high-altitude-wind-turbine-03-24-2014/

Bartholomė, E, and A Belward. “The Availability of Renewable Energies in a Changing Africa .” JRC Scientific and Policy Reports, 2013.

Bartosik, Gill, Lybarger, Nyren, Wilder. Design of a Kite-Powered Water Pump and Airborne Winds Turbine. Diss. Worcester Polytechnic Institute, 2012.

Bauer, Beauchemin, Draper, Munene, Blarcum, Zhao. Redesign of the WPI Rotary Kite-Powered Water Pump. Diss. Worcester Polytechnic Institute, 2016.

“BIRDY Certified Rear Rack Ezwheels.” BikeGang, bikegang.ecwid.com/#!/BIRDY-Certified-Rear-Rack-Easy-wheels-Multi-S/p/43695878.

Blarcum, Jon Van. Collapsible Kite Powered Water Pump. MS Directed Research Report, 2016.

Blouin, Michael, Benjamin Isabella, and Joshua Rodden. "Wind Power from Kites." MQP, Worcester Polytechnic Institute April 26 (2007).

Buckley, Ryan, et al. "Design of a One Kilowatt Scale Kite Power System." MQP/DJO 308 (2008).

Cartier, Adam, et al. Re-Design and Testing of the WPI Kite Power System. Diss. Worcester Polytechnic Institute, 2010.

Caula, R. (2014, March 24). Altaeros energies high altitude wind turbine deploys at 1,000 feet. *Designboom*. From https://www.designboom.com/technology/altaeros-energies-high-altitude-wind-turbine-03-24-2014/

Chase, DeLuca, Marshall, Mazurkiewicz. Design and Testing of Kite-Powered Water Pump Concepts. Diss. Worcester Polytechnic Institute, 2015.

Cherubini, A., Papini, A., Vertechy, R., & Fontana, M. (2015). Airborne Wind Energy Systems: A Review of the Technologies. *Renewable and Sustainable Energy Reviews, 51*. From http://dx.doi.org/10.1016/j.rser.2015.07.053

Diehl, M. (2013, October 2). Airborne Wind Energy: Basic Concepts and Physical Foundations. In *Green Energy and Technology* (1). From file:///C:/Users/Zeb/Downloads/springerchapter1%20(2).pdf

Falkenmark, M. (1989). The Massive Water Scarcity Now Threatening Africa: Why Isn't It Being Addressed? *Ambio, 18*(2), 112-118. Retrieved May 25, 2017.

Frewin, Jimenez, Roth. Design of a Remote Controlled Tether System for the WPI Kite Power System. Diss. Worcester Polytechnic Institute.

Gagliano, Marsh, Long. Design of a Two- Kite Rotary Power Cycle for the WPI Kite-Powered Water Pump. Diss. Worcester Polytechnic Institute, 2016.

“Global Water Shortage: Water Scarcity & How to Help - Page 2.” The Water Project, thewaterproject.org/water-scarcity/water_scarcity_2#phys.

Johnston Environment Correspondent, Ian. “Developing World Invests More in Renewable Energy than Rich Countries for First Time, New Study Says.” The Independent, Independent Digital News and Media, 31 May 2016, www.independent.co.uk/environment/climate-change/renewable-energy-investment-developed-world-developing-world-ren21-report-a7058436.html.

Lansdorp, B., & Ockels, W. J. (2005). *Comparison of Concepts for High-Altitude Wind Energy Generation with Ground Based Generator*. From http://edge.rit.edu/edge/P14462/public/Working%20Documents/Research/P14462%20-%20Lansdorp%20-%202005%20-%20Comparison%20of%20concepts%20for%20high-altitude%20wind%20energy%20generation%20with%20ground%20based%20generator.pdf

Lansdorp, B., & Ockels, W. J. (Authors of document). (2005). *Pumping mill* [Cropped drawing]. From http://edge.rit.edu/edge/P14462/public/Working%20Documents/Research/P14462%20-%20Lansdorp%20-%202005%20-%20Comparison%20of%20concepts%20for%20high-altitude%20wind%20energy%20generation%20with%20ground%20based%20generator.pdf

Lansdorp, B., & Ockels, W. J. (Authors of document). (2005). *The Laddermill concept* [Cropped drawing]. From http://edge.rit.edu/edge/P14462/public/Working%20Documents/Research/P14462%20-%20Lansdorp%20-%202005%20-%20Comparison%20of%20concepts%20for%20high-altitude%20wind%20energy%20generation%20with%20ground%20based%20generator.p df

N. Lakshmanan, S. Gomathinayagam, P. Harikrishna, A. Abraham and S. Chitra Ganapathi. "Basic Wind Speed Map of India with Long-Term Hourly Wind Data ." www.sefindia.org/forum/files/wind_loading_map_630.pdf.

"National Kite Month April 1st – 30th, 2017." *National Kite Month*, American Kite, www.nationalkitemonth.org/how-to-fly-a-kite/.

Occupational Safety and Health Administration (n.d.). *Protective Measures to Take at Each Risk Level*. From https://www.osha.gov/SLTC/heatillness/heat_index/protective_high.html

Occupational Safety and Health Administration (n.d.). *Protective Measures to Take at Each Risk Level*. From https://www.osha.gov/SLTC/heatillness/heat_index/protective_veryhigh.html

Shepard, B. (Artist). (n.d.). *Flying Electric Generator* [Artist's rendition], From http://www.skywindpower.com/ww/index.htm.

Sky WindPower (n.d.). Potentially Our Cheapest Energy Source. In *High Altitude Wind Power* (Home). From http://www.skywindpower.com/ww/index.htm

Toydemir, C. Kuthan. Design of a Dynamometer for the WPI Kite Power System. Diss. WORCESTER POLYTECHNIC INSTITUTE, 2010.

piotr (2009, November 20). *Getting Wind Power Off the Ground*. From http://etcgreen.com/getting-wind-power-off-the-ground/

Werber, C. (2016, June 1). The developing world is outspending richer countries on renewable energy investment. *Quartz Media LLC*. From https://qz.com/696642/renewable-energy-just-had-its-best-year-ever-thanks-to-developing-countries/

“Water.” *United Nations*, United Nations, www.un.org/en/sections/issues-depth/water/.